Artificial Intelligence in Upper Limb Robot-Aided Physical Rehabilitation: A Systematic Review

RITA MOLLE, Research Unit of Advanced Robotics and Human-Centred Technologies, Università Campus Bio-Medico di Roma, Rome, Italy
CHRISTIAN TAMANTINI, Institute of Cognitive Sciences and Technologies, National Research Council of Italy, Rome, Italy
LOREDANA ZOLLO, Research Unit of Advanced Robotics and Human-Centred Technologies, Università Campus Bio-Medico di Roma, Rome, Italy

Rehabilitative therapies play a crucial role in upper limb motor recovery, as upper limbs are the most active parts in executing the activities of daily living. Because of a huge number of people with motor disorders and a shortage of therapists, the integration of data-driven AI methodologies and robots for rehabilitation could be helpful in creating personalized and challenging therapies, leading to a myriad of benefits for both patients and therapists. AI methods can be implemented in different functional modules of the robotic platform, such as user intention recognition, robot motion planning, robot interaction control, and system adaptation through different learning paradigms. This article presents a systematic literature review on the use of data-driven learning methods applied in upper limb robot-aided rehabilitation. The analysis is structured around the learning paradigms adopted, namely, supervised, unsupervised, and reinforcement learning, as well as the corresponding task types (e.g., classification, regression, and control tasks) and model types, distinguishing between machine learning and deep learning approaches. The review reveals that most studies employ supervised learning to address classification tasks, and that deep learning models are the most frequently adopted.

CCS Concepts: • **Information systems** → **Information systems applications**; • **Computing methodologies** → **Artificial intelligence**; **Machine learning**; • **Applied computing** → **Life and medical sciences**;

Additional Key Words and Phrases: Artificial Intelligence, Machine Learning, Deep Learning, upper limb rehabilitation, robot-aided rehabilitation, user intention recognition, robot motion planning, robot interaction control, system adaptation

ACM Reference format:
Rita Molle, Christian Tamantini, and Loredana Zollo. 2026. Artificial Intelligence in Upper Limb Robot-Aided Physical Rehabilitation: A Systematic Review. *ACM Trans. Hum.-Robot Interact.* 15, 2, Article 41 (January 2026), 35 pages.
https://doi.org/10.1145/3779302

This work was supported by the Italian Ministry of Research, under the complementary actions to the NRRP "Fit4MedRob—Fit for Medical Robotics" Grant (PNC0000007) (CUP: B53C22006990001).

Authors' Contact Information: Rita Molle (corresponding author), Research Unit of Advanced Robotics and Human-Centred Technologies, Università Campus Bio-Medico di Roma, Rome, Italy; e-mail: rita.molle@unicampus.it; Christian Tamantini, Institute of Cognitive Sciences and Technologies, National Research Council of Italy, Rome, Italy; e-mail: christian.tamantini@cnr.it; Loredana Zollo, Research Unit of Advanced Robotics and Human-Centred Technologies, Università Campus Bio-Medico di Roma, Rome, Italy; e-mail: l.zollo@unicampus.it.

ACM 2573-9522/2026/1-ART41
https://doi.org/10.1145/3779302

1 Introduction

Rehabilitation plays a crucial role in helping individuals recover from injuries, surgeries, or medical conditions. The rehabilitation of the upper limb is more important for self-care ability, as the upper limbs are the most active parts of the human body [1]. Neurological and musculoskeletal disorders, for example, can affect the upper limbs, leading to difficulties with **Activities of Daily Living (ADLs)**. The regain of the lost capabilities in performing ADLs can be executed with conventional manual therapy, but due to a large number of patients, this type of therapy cannot meet the huge need and suit different individual situations of patients [2]. Moreover, conventional treatments rely on the operator's judgment and involve semi-qualitative assessments. For these reasons, technological advancements have revolutionized the field of rehabilitation, with robotics emerging as a powerful tool to assist in the recovery process [3]. In the last decade, different studies were carried out in order to prove the effectiveness of robot-aided rehabilitation for the treatment of patients affected by upper limb disorders of the neuromuscular [4] and musculoskeletal systems [5].

The introduction of robotic technology for physical interaction in the clinical field has offered a myriad of benefits for patients on their journey to recovery [6, 7]. By objectively measuring the patient's motor performance [8], enhancing sensorimotor training [9], increasing intensity [10], fostering active participation and engagement [11], as well as promoting independence and accessibility [12], robotics has become of paramount importance for modern rehabilitation practices providing tailored and personalized therapy [13].

The integration of AI into robot-aided rehabilitation further enhances the potential of these systems, bringing rehabilitation closer to the goals of precision medicine. AI allows the extraction of meaningful patterns from large volumes of heterogeneous data, such as kinematic and dynamic variables from robots, and biosignals, to support adaptive, data-driven therapy [14]. Unlike traditional systems, AI-based solutions can continuously monitor the patient's state, adjust assistance strategies in real time, and personalize the treatment pathway based on each individual's progress and needs [15, 16]. This capability makes AI essential for delivering intelligent and responsive rehabilitation interventions.

Data-driven AI approaches encompass a range of methods designed to extract actionable insights from the continuous stream of data generated during therapy. These include supervised learning paradigms applied to classification and regression tasks, aiming to assess patient status or predict recovery trajectories; unsupervised learning techniques, such as clustering, to reveal hidden patterns or identify subgroups of patients with similar profiles; and **Reinforcement Learning (RL)**, which enables the system to learn optimal policies by refining the robot's behavior in real time through interaction with the environment. These learning paradigms, implemented through various model types, including statistical models, neural networks, or hybrid frameworks, contribute to constructing a dynamic and personalized representation of the user, ultimately enabling more adaptive and effective rehabilitation interventions. The analysis presented in this review focuses on how each learning paradigm is implemented and evaluated in the literature, offering a structured overview of the role of data-driven models in enabling intelligent and adaptive rehabilitation.

The objective of this review is to provide a comprehensive systematization of existing studies on the application of data-driven learning approaches within the field of AI in upper-limb robot-aided rehabilitation therapy, encompassing both end-effector and exoskeleton-based systems. Actually, although many literature reviews have addressed several aspects of robot-aided rehabilitation focusing their attention on separately robot aspects, such as **Robot Motion Planning (RMP)** [17], human–robot interaction modalities [18], robot control strategies [19, 20], **Electromyography (EMG)**-based motor intention prediction [21], AI application in mobile robotic exoskeletons [20, 22], **Deep Learning (DL)** application for EMG-based Human–Machine Interaction [23], interactive design on exoskeleton performance [24], design and application of **Machine Learning (ML)** in robot-aided upper limb rehabilitation [25], and automated planning and scheduling application in healthcare [26], this article wants to provide a comprehensive analysis of all the studies in the literature regarding the integration of AI methodologies in upper-limb robot-aided rehabilitation. Compared to previous reviews, the novelty of this article lies in providing a structured summary of the main data-driven AI techniques employed in the management of robot-aided rehabilitation therapy, covering key functional areas such as RMP and control, **User Intention Recognition (UIR)**, and therapy adaptation based on individual user needs. It has been demonstrated that the adoption of AI in upper limb robot-aided rehabilitation can be useful for many purposes. It allows exploring the movement patterns [27], predicting human intentions [28], controlling the robotic devices (exoskeleton or end-effector) [29], providing sensory feedback to the patient through a **Virtual Reality (VR)** system [30] or seeing the motion of the impaired limb through the activation of the robotic device [1]. Furthermore, it enables estimating the user's state by analyzing physiological signals, thus adapting the robot behavior, accordingly [5], ensuring enhanced customization and personalization of the rehabilitation session.

This review aims to address key research questions concerning the role of data-driven AI in robot-aided rehabilitation systems, including:

Q1: the identification of functional modules that currently incorporate AI algorithms and how these modules are defined across the literature;

Q2: the examination of data-driven learning methodologies applied to specific tasks within these modules;

Q2: the analysis of performance metrics and evaluation strategies used to assess the effectiveness of AI methods, with attention to their consistency across studies.

This review article wants to address these research issues through a systematic analysis of the current landscape, identifying existing gaps, and proposing future directions to foster the effective and responsible deployment of AI in robot-aided rehabilitation. Moreover, it evaluates the complexity of the AI algorithms applied in different rehabilitation settings, the type of data fed in the AI module, and the population enrolled for the validation purpose.

The article is organized as follows. Section 2 describes the method used for literature analysis. Section 3 reports the existing AI algorithms applied in the robotic rehabilitative field for robotic therapy management. This section is divided into four subsections according to the functional block that implements an AI algorithm. Section 4 discusses the main results that emerged from the literature analysis, and Section 5 provides the conclusions of the present article.

2 Methods

A comprehensive literature search, updated to December 2024, was conducted using Google Scholar, Scopus, and IEEE Xplore. Specifically, the following query was implemented in the scientific databases: "robot*" *AND* "upper limb rehabilitation" *AND* ("artificial intelligence" *OR* "machine learning" *OR* "deep learning" *OR* "reinforcement learning"). The logic operators have been included to ensure that each paper includes the presence of the robot, the upper limb rehabilitation scenario, and the application of an AI-based methodology. Additionally, the use of * ensures to broaden the search by finding words that start with the same letters (e.g., robot, robots, robotics). Moreover, to include relevant papers, the following inclusion criteria were utilized:

- All the publications should be written in English and published in the period between 2010 and 2024;
- All the papers and conference articles should be indexed on Scopus;

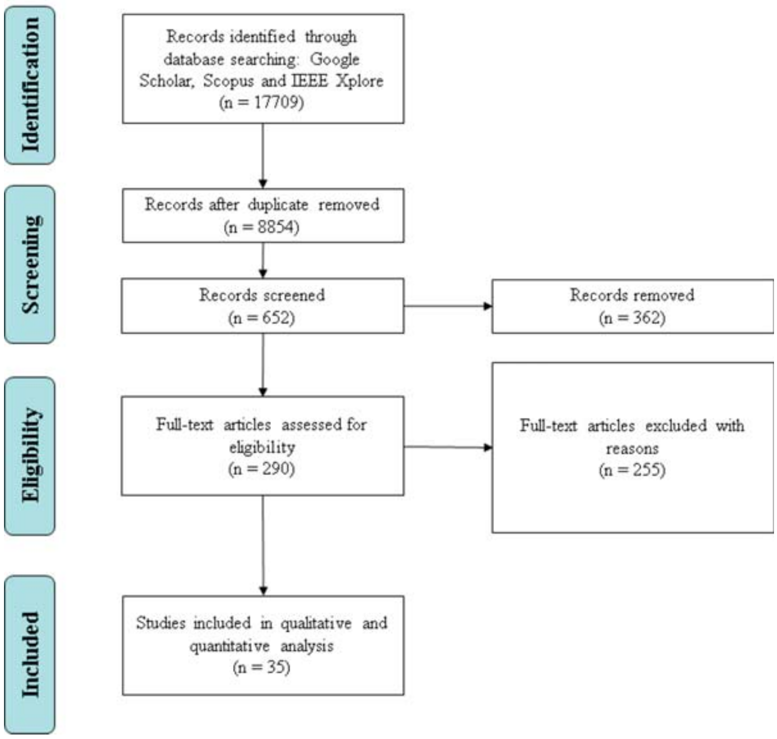

Fig. 1. PRISMA flowchart of the search and inclusion process.

- The papers should concern upper limb rehabilitation with a robotic device including both the exoskeleton and the end-effector;
- The papers should concern upper limb rehabilitation with a robotic device integrating an AI algorithm in one of its functional blocks. The AI module should not be used as a method of evaluation or assessment. This choice was made to focus on studies where AI directly supports real-time control or adaptation of the rehabilitation process. Although assessment methods can indirectly contribute to adaptive control, the review includes only those integrating AI within the control or therapy adjustment loop;
- The adopted AI approach must be clearly specified by indicating the learning paradigm, the task type, and the specific algorithm used. Generic references to ML or DL as model types are not sufficient; the exact model should be described to ensure transparency and repeatability.

The search strategy was based on **Preferred Reporting Items for Systematics Reviews and Meta-Analysis (PRISMA)** statement [31]. The documents obtained were screened to ensure that eligibility criteria were met.

3 Results

The resulting PRISMA is shown in Figure 1. The systematic review process started with the identification of 17,715 documents in the search stage. After removing duplicates, 652 papers were analyzed. 362 papers were excluded based on a comprehensive review of the abstracts and the entire paper, which determined that they did not meet the established inclusion criteria. In particular:

— 10 theses were excluded;
— 20 works were excluded because the proposed therapy was not for the upper limb;
— 19 works were excluded because they did not deal with rehabilitation;
— 64 works were excluded because there was not any robotic device;
— 150 papers were excluded because there was no application of an AI algorithm in one of the functional blocks;
— 33 papers were excluded because the AI method integrated into the robotic device was not described;
— 66 papers were excluded because the AI method was used for patient evaluation or assessment purposes.

The remaining 290 papers were fully reviewed; however, 255 were excluded for several reasons. Many involved robotic devices such as pneumatic artificial muscles or prostheses, which do not fall within the scope of end-effector or exoskeleton systems. Additionally, some studies did not clearly describe the implemented AI module, lacking details such as the number of layers in the neural networks or the hyperparameters used. Preference was also given to studies applying AI methods to address specific task types such as classification, regression, or control, within a data-driven learning paradigm, as these represent the most commonly used approaches in the field.

This search and screening process led to the identification of 35 relevant studies. To address research question *Q1*, we developed a functional schematic of upper-limb robot-aided rehabilitation architectures based on the analysis of these works. This diagram, presented in Figure 2, illustrates the system modules identified in the literature and highlights which of them integrate AI algorithms, thereby clarifying their specific roles within the overall rehabilitation framework. At the human–robot interaction level, a patient monitoring system can be exploited to monitor the relevant parameters to provide insight into the patient's state. Multi-modal sources of information can be fed into UIR algorithms that aim at estimating the patient's motion intention. The output of this functional block can be the starting point for the robotic system intervention in order to meet the user's needs. Specifically, RMP and **Robot Interaction Control (RIC)** characterize robot behavior in terms of trajectory planning and physical interaction. Moreover, the robotic system parameters can be tuned according to the output of algorithms devoted to the **System Adaptation (SA)**. In this way, tailoring the behavior of the robot as well as providing feedback in real-time to the specific patient's needs is possible to promote patients' motor outcome and engagement [32]. The functional blocks reported in Figure 2 can implement AI approaches for physical therapy in rehabilitation, the focus of this review. For this reason, the papers selected for the review are organized based on their specific proposed application: 15 for UIR, 8 for RMP, 6 for RIC, and 7 for SA. It is worth noticing that the paper [33] has been included both in UIR and SA as there are two different AI modules applied in two different functional blocks.

To address *Q2* and *Q3* (i.e., the examination of data-driven learning methodologies applied to specific tasks within the identified functional modules, and the analysis of performance metrics and evaluation strategies used to assess the effectiveness of AI methods), a thorough review of the selected papers is required. Since these aspects can only be meaningfully analyzed after a detailed examination of each study methodological framework, learning paradigm, and validation process, the discussion of these research questions is deferred to the Discussions section (Section 4).

For this purpose, each paper selected in the search stage has been carefully reviewed to extract the most relevant information regarding:

— the signals acquired during the experiments: EMG for muscle activity, kinematics data coming from magneto **Inertial Measurement Units (IMUs)**, cerebral activity monitored with

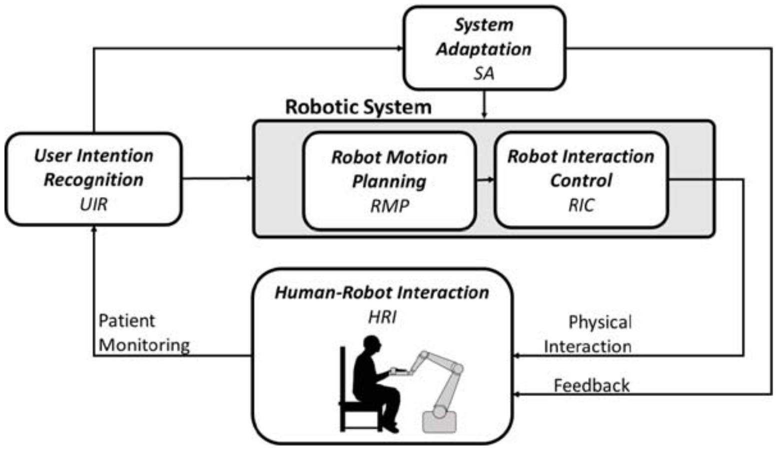

Fig. 2. Functional scheme of an AI-driven upper limb robot-aided rehabilitation system, highlighting the main modules: UIR, RMP, RIC, and SA.

Electroencephalogram (EEG), **Heart Rate (HR)**, **Respiration Rate (RR)**, skin Temperature (T), **Galvanic Skin Response (GSR)**;
- the subjects included in the study, divided into healthy (H) or patients (P). The pathology is expressed if there is P;
- dataset and software information, including **Dataset Size (DS)**, **Dataset Availability (DA)**, and source **Code Availability (CA)**. When this information is not provided, the entry is marked as **Not Applicable (NA)**;
- the robot used in the experiments: if the robot is a commercial one or it is a research prototype;
- the learning paradigm adopted in the study: supervised learning (further distinguished by the task type, such as Classification (C) or Regression (R)), unsupervised learning, or RL), which is typically associated with control (Ctrl) or policy optimization tasks. In this context, control refers to the continuous regulation of relevant robot variables;
- the specific AI algorithm used, from which the model type (ML or DL) can be inferred. If the study includes a comparative analysis of multiple models, only the best-performing algorithm is reported;
- all relevant details regarding the hyperparameters used in each AI algorithm, including the number of training epochs, the architecture of DL models, and other key configuration parameters;
- the output generated by the AI algorithm, which indicates the task type addressed. For classification tasks, all possible classes are explicitly listed;
- the validation strategy used to evaluate the performance of the proposed algorithm. Common strategies include **Leave-One-Subject-Out (LOSO)** and **Leave-One-Out Cross-Validation (LOOCV)**;
- the performance metrics reported in the study, which may include Accuracy (Acc), **Area Under the Curve (AUC)**, F1-score, **Mean Absolute Error (MAE)**, correlation coefficient, coefficient of determination (R^2), **Mean Square Error (MSE)**, and **Root MSE (RMSE)**.

For each subsection, all information has been summarized in a specific table: Table 1 for UIR, Table 2 for RMP, Table 3 for RIC, and Table 4 for SA.

Table 1. AI Approaches in Robot-Aided Rehabilitation for UIR

	Signals	Subjects	Data	Robot	Task: Algorithm	Hyperparameters	Prediction	Validation	Performance
[36]	EMG	5H	DS: NA DA: private, NA CA: NA	Exoskeleton: Research prototype	C (2 cl): SVM	Soft margin method Gaussian kernel function epochs length: 200 ms	Joint state (movement or rest)	10 fold cross-validation	AUC: 90.00%
[37]	EMG	28H	DS: 28 healthy subjects; 7 movements × 20 repetitions each; total 3,920 segmented EMG signal sets DA: private, NA CA: NA	Exoskeleton: Research prototype	C (4 cl): SVM	Polynomial kernel Optimized: Bayesian Optimization epochs length: 135 ms	Shoulder motion pattern (drinking, opening a door, abducting, resting)	80% training set; 20 % test set	Acc: 90.00%
[38]	EMG	5H	DS: NA DA: private, NA CA: NA	ReRobot	C (4 cl): SVM	Radial basis kernel function Optimized $C = 0.4579$ Optimized $\sigma = 371.6339$ epochs length: 128 ms	Upper limb motion pattern (shoulder flexion, abduction, internal rotation, external rotation, and elbow joint flexion)	10 five-fold cross-validation	F1-score: 93.68%
[33]	EMG	10H	DS: NA DA: private, NA CA: NA	End-effector: Research prototype	C (3 cl): PSO-SVM	Radial basis kernel function Particle Swarm Optimization epochs length: 200 ms	Recovery state (active, passive, and resistive training mode)	90% training set, 10% test set	Acc > 93.98%
[39]	EMG, IMU	10H	DS: NA DA: private, NA CA: NA	Exoskeleton: Research prototype	C (2 cl): DT	Epochs: 100 samples	EMG pattern recognition (arm joint flexion and extension movement)	80% training set, 20% test set	Acc: 96.36%
[40]	EMG, motion data	10H	DS: NA DA: available at CA: available at	End-effector: Research prototype	C (2 cl): DT	Criterion: Gini Splitter: best Min samples split: 2 Min samples leaf: 1 CCP alpha: 0.0	Intention of movement (pre-intention and intention)	70% training set, 15% validation set, 15% test set	Acc: 99.00%
[41]	EMG	8H	DS: NA DA: private, NA CA: NA	Exoskeleton: Research prototype	C (10 cl): ANN	10 hidden layers Architecture: 2-processing blocks scaled conjugate gradient backpropagation neural network (Block 1: netsum + tansig; Block 2: netsum + softmax)	Hand gesture recognition (radial deviation, ulnar deviation, wave in, wave out, relax, pinky flexion, pinky extension, grasp a bottle, bottle/pinky flexion, bottle/pinky extension)	Split validation	Acc: 93.00%

(Continued)

Table 1. Continued

	Signals	Subjects	Data	Robot	Task: Algorithm	Hyperparameters	Prediction	Validation	Performance
[34]	EMG	2H	DS: 250 samples (after feature extraction and dimensionality reduction via PCA) DA: private, NA CA: NA	Exoskeleton: Research prototype	C (5 cl): BPNN	3 layers: input layer (16 nodes), hidden layer (10 nodes), output layer (5 nodes) Training samples: 50-125 Training repetitions: Each configuration tested over 30 independent runs Selection: Hidden nodes tested from 5 to 24 Ensemble: Boosting-based method to combine weak classifiers	Arm motion (shoulder extension/flexion, shoulder abduction/adduction, elbow extension/flexion, eating, lifting trousers)	Multiple train-test runs (30 repetitions) with varying training sample sizes to assess convergence and generalization	Acc: 95.50%
[42]	EMG	8H	DS: three-channel analysis windows containing motion intent information and 192 × 3 = 576 data points DA: private, on reasonable request CA: on reasonable request	Robotic arm	C (6 cl): Lw-CNN	Conv1: 16 filters, 3×3, stride 1, padding "same" Conv2: 32 filters, 3×3, stride 1, padding "same" MaxPooling: 2×2 after each conv block Activation: ReLU Normalization: Batch-Normalization Dropout: 0.5 Output: Softmax Params: ~367k Input window: 192 ms	Upper limb motion pattern (elbow flexion, elbow extension, shoulder flexion, shoulder extension, elbow & shoulder flexion, and elbow and shoulder extension)	80% training set, 20% test set	Acc: 88.75%
[43]	EMG	10H, 4P (spinal cord injury)	DS: NA DA: private, NA CA: NA	Exoskeleton: Research prototype	C (2 cl or 4 cl): LDA	Combination with Recursive Feature Elimination with Cross Validation epochs length: 200 ms Solver: svd Tol: 1e-4	Intended direction of movement (elbow flexion/extension, forearm pronation/supination, wrist flexion/extension, and wrist radial/ulnar deviation; elbow flexion/extension combined with forearm pronation/supination and wrist flexion/extension combined with wrist radial/ulnar deviation)	5-fold cross-validation during training with minimum accuracy criteria (≥85% per fold, mean ≥95%). Testing performed on unseen data with and without robot motion feedback using 10 repetitions per direction	Acc single-DoF control mode: 85.00–95.00%, Acc multi-DoF control mode: 60.00%

(Continued)

Table 1. Continued

	Signals	Subjects	Data	Robot	Task: Algorithm	Hyperparameters	Prediction	Validation	Performance
[45]	EEG	15H	DS: 240 trials per subject. EEG signal: 20 × 400 (channel × time) DA: private, NA. Video at CA: NA	JACO arm	C (6 cl): MDCBN	Input: 20×400 (EEG channel×time) CNN: 3 conv layers (1×10, 20×1 filters), pooling 1×3 BiLSTM: 300 hidden units, dropout 0.5, forward & backward FC: ReLU, regression output per 3D velocity Epochs: 500, best model saved by test loss	Intuitive imagery for 6 directions of motion	subject-dependent; 80% training set, 20% test set	Acc of the online experiments: 60±14% and 43±9%
[46]	EEG	6H	DS: 9 subjects × 256 trials (public); 6 subjects × 6 sessions × 100 trials (private) DA: private and public BCI Competition IV 2a and 2b CA: available at	End-effector: Research prototype	C (4 cl): STFCN	Blocks: Spatial-Conv; Temporal-Conv; FC Layers: Conv + BN + Leaky ReLU ($\alpha = 0.2$) Dropout: 0.3 Activation: Leaky ReLU with slope $\alpha = 0.2$ Spatial Conv: 16 ch, kernel $(L, 1)$, stride $(L, 1)$ Temporal Conv 1: 32 ch, kernel $(1, 23)$, stride $(1, 3)$ Temporal Conv 2: 64 ch, kernel $(1, 17)$, stride $(1, 1)$ + MaxPool $(1, 6)$ Temporal Conv 3: 128 ch, kernel $(1, 7)$, stride $(1, 1)$ + MaxPool $(1, 2)$ Final: Flatten → FC → Leaky ReLU → Dropout	Movement direction (forward, backward, left, right)	Offline: 80% training set, 20% test set Online: test of the trained model	Acc of the online experiments: 62.70%
[47]	EEG	5H	DS: 2,160 samples (360 target, 1,800 no-target) DA: private, on reasonable request CA: on reasonable request	End-effector: Research prototype	C (2 cl): SVM	Non-linear kernel	Human intention (Target meant P300 signal detected; No Target meant P300 signal detected)	5-fold cross-validation	Acc: 80.83%

(Continued)

Table 1. Continued

	Signals	Subjects	Data	Robot	Task: Algorithm	Hyperparameters	Prediction	Validation	Performance
[44]	EEG	7H	DS: 62 × 18 DA: private, NA CA: NA	End-effector: Research prototype	C (3 cl): CNN	Number of convolutional layers: 2 Number of kernels in the first layer: 50 Number of kernels in the second layer: 100 Kernel size: 4 × 4 Pooling: max pooling with size 2 × 2, non-overlapping Activation function in convolutional layers: ReLU Activation function in hidden layer: Sigmoid Activation function in output layer: Softmax Dropout in convolutional layers: 15% retention rate	Movement intention (supination/pronation of the forearm, flexion/extension of the arm, rest)	80% training set, 20% test set	Acc: 68.00 ± 15.00%
[48]	EEG, gaze	3H, 4P (stroke)	DS: 80 trials, 40 for each task DA: private, NA CA: NA	Light-Exos	C (2 cl): SVM	NA	Movement intention (movement and rest)	Training on visual condition (virtual arm); tested on robot condition (real exoskeleton)	Acc: 89.40 ± 5.00%

In the “Subjects” column, the healthy (H) and pathological (P) conditions of the enrolled subjects are reported. In the “Data” column, dataset size (DS), data availability (DA), and code availability (CA) are reported. When this information is not provided, the entry is marked as not applicable (NA). In the “Task: Algorithm” column, the task type is specified according to the learning paradigm. For supervised learning, task types include Regression (R) and Classification (C); in the case of classification, the number of classes is indicated in parentheses and followed by the acronym “cl.” For reinforcement learning, the task type is specified as control (Ctrl). In the same column, the specific algorithm used to address the task is also reported: Support Vector Machine (SVM), Particle Swarm Optimization (PSO)-SVM, Decision Tree (DT), Artificial Neural Network (ANN), BackPropagation Neural Network (BPNN), Lightweight Convolutional Neural Network (Lw-CNN), Linear Discriminant Analysis (LDA), Multi-Directional Convolutional Neural Network (CNN) Combined with a Bidirectional Long Short-Term Memory (BiLSTM) Network (MDCBN), Spatial-Temporal Filtering Convolutional Neural Network (STFCN), Convolutional Neural Network (CNN). In the “Hyperparameters” column, C is the Penalty Factor, σ is the Kernel Function Parameter, FC Indicates Fully Connected Layer, BN Indicates Batch Normalization, NA (Not Applicable). In the “Performance” column, AUC Indicates Area Under Curve and Acc Indicates Accuracy.

Table 2. AI Approaches in Robot-Aided Rehabilitation for RMP

	Signals	Subjects	Data	Robot	Task: Algorithm	Hyperparameters	Prediction	Validation	Performance
[55]	Torque and position	-	DS: NA DA: private, NA CA: NA	Simulated end-effector: Research prototype	Ctrl: DPPO	Penalty coefficient: mitigates large policy changes Number of parallel actors/threads: uses a distributed setup (NA) Learning rate: implicitly tuned (regularized via DPPO updates) Batch size/rollout length: not explicitly given (PPO-based) Reward shaping: dense reward functions (azimuth + aspiration) to accelerate convergence	Optimized rehabilitation robot trajectory	Simulation: based on convergence rate, mean value, and standard deviation	Reward: 1,970.60, Episodes: 258
[49]	Force	2H	DS: NA DA: private, NA CA: NA	End-effector: Epson E2L853	R: Neuro-fuzzy	Fuzzy sets: trapezoidal membership functions (antecedents) Number of crisp inputs: 2 Rule activation: product of membership degrees $B_{ij}(x_{0j})$ Learning type: online gradient descent Loss function: Mean Squared Error	Real-time patient-specific rehabilitation trajectory generation	Validation based on tracking error	max MSE: 0.12 m
[50]	EMG, IMU	11H	DS: EMG features = 10×16 feature matrix per sample DA: private, NA CA: NA	NTUH-II	R: MS-LSTM Dueling	Inputs: human arm dynamics (joint angles, velocities, accelerations) from IMU sensors; EMG features extracted Architecture: two streams—LSTM for dynamics data, ConvLSTM for sEMG data to capture spatial correlations	Joint angles	Offline: training on 3 subjects (5 sessions each), validation on remaining sessions; testing on 5 separate subjects. Online: 3 subjects	MAE: 0.97
[51]	Motion data	4H	DS: NA DA: private, NA. Video at CA: NA	Exoskeleton: Research prototype	R: CNN-LSTM	Conv1D(1): Filters = 80, kernel_size = 1, padding = valid MaxPooling1D(1): Pool_size = 2, padding = valid Conv1D(2): Filters = 48, kernel_size = 1, padding = valid MaxPooling1D(2): Pool_size = 1, padding = valid Dropout(1): Rate = 0.2 LSTM(1): Units = 32 LSTM(2): Units = 16 Dropout(2): Rate = 0.2 Dense(1): Units = 64 Dense(2): Units = 1	Elbow and wrist angles	Training on subjects' motion data and comparison with a baseline	R^2 task 1: 0.93, R^2 task 2: 0.91

(Continued)

Table 2. Continued

	Signals	Subjects	Data	Robot	Task: Algorithm	Hyperparameters	Prediction	Validation	Performance
[1]	EMG	10H	DS: NA DA: private, NA CA: NA	PVSED	R: BPNN	3 layers (input, 1 hidden, output) Input units: 18 Hidden units: 38 Output units: 1 Activation function: Sigmoid in hidden layer, linear in output layer epochs length: 200 ms	Elbow joint angle	Offline training with Leven-berg–Marquardt (70% training set, 30% test set) and real-time testing on bilateral synchronization	ρ: 90.00% RMSE: 0.36 rad
[52]	EMG, motion data	10H	DS: 60,000 sliding windows from 10 subjects (5 sessions each), 8-channel EMG data per window DA: private, NA CA: NA	Exoskeleton: Research prototype	R: CNN-LSTM	15 layers Layers: Input layer (50 × 1), sequence folding layer, convolutional, batch normalization, ELU, Average Pooling 2 D, Sequence Unfolding, Flatten, LSTM (128 hidden units), Dropout (0.25), LSTM (32 hidden units), Dropout (0.25), 2 fully connected, regression output layer epochs length: 200 ms	Elbow joint angle	70% training set, 30% test set	R^2: 0.93
[53]	Motion data	1H	DS: 5 demonstrations per movement, each as 4 joint-space trajectories DA: private, NA CA: NA	Exoskeleton: Research prototype	R: HMM	NA	Trajectories	Validation based on therapist's judgment	Agreement: 70.40%
[54]	Motion data	1H	DS: NA DA: private, NA CA: NA	Exoskeleton: Research prototype	R: ProMP	Input: Multiple demonstrations of joint trajectories (positions and velocities) Radial basis functions Weights learned from demonstrations	Trajectories	Comparison with Dynamic Movement Primitives on motion data, evaluated by smoothness, velocity, acceleration, and curvature metrics	Jerk: 22.56

In the "Subjects" column, the Healthy (H) and Pathological (P) conditions of the enrolled subjects are reported. In the "Data" column, Dataset Size (DS), Data Availability (DA), and Code Availability (CA) are reported. When this information is not provided, the entry is marked as Not Applicable (NA). In the "Task: Algorithm" column, the task type is specified according to the learning paradigm. For supervised learning, task types include Regression (R) and Classification (C); in the case of classification, the number of classes is indicated in parentheses and followed by the acronym "cl." For RL, the task type is specified as Control (Ctrl). The same column also reports the specific algorithm used to address the task: Distributed Proximal Policy Optimization (DPPO), Multi-Stream Long Short Term Memory Dueling (MS-LSTM Dueling), Convolutional Neural Network—Long Short Term Memory (CNN-LSTM), BackPropagation Neural Network (BPNN), Hidden Markov Models (HMM), Probabilistic Movement Primitives (ProMP). In the "Hyperparameters" column, NA indicates Not Applicable. In the "Performance" column, MSE, RMSE, MAE, ρ, and R^2 indicate mean square error, root mean square error, mean absolute error, correlation coefficient, and coefficient of determination, respectively.

Table 3. AI Approaches in Robot-Aided Rehabilitation for RIC

	Signals	Subjects	Data	Robot	Task: Algorithm	Hyperparameters	Prediction	Validation	Performance
[29]	IMU	-	DS: NA DA: private, NA CA: NA	Bilateral robot: Research prototype	R: RBF neural network	3 layers Gradient descent method Learning rate = 0.8	Movement trajectory of the affected side limb	60% training set 40% test set	Max angular error: 0.09 rad
[57]	Mechanical impedance parameters	-	DS: NA DA: private, NA CA: NA	Simulated robot: Research prototype	R: EDRFNN	Membership functions: 7 Gaussian Structure: 5 layers—Input, Membership, Rule, Normalization, Output	Desired impedance control parameters	Validation based on task performance and tracking error	Time regulation: 0.21 s, Tracking error: $-0.17 \pm 2.29 \times 10^{-2}$ m
[58]	Motion data	-	DS: NA DA: private, NA CA: NA	iTbot	Ctrl: DDPG	Architecture: Deep neural networks for both actor and critic	Control parameters for tracking therapeutic trajectories	Simulation: random input signals to ensure generalization	Max tracking error: 0.16 rad
[59]	Interaction force	5H	DS: NA DA: private, NA CA: NA	Simulated end-effector: Research prototype	Ctrl: NN-based AC learning	NA	Control actions for trajectory tracking on rehabilitation robot	Simulation and real-robot experiments Lyapunov-based stability proof	Position error: 0.05 rad
[60]	Force, Torque	1H, 2P (stroke)	DS: NA DA: private, NA CA: NA	Exoskeleton: Research prototype	R: RBF neural network	Gaussian function Control parameters: $\Lambda = [6.6,\ 10,\ 6.8,\ 7.5,\ 6.3,\ 4.2,\ 3.6]$ $\eta = 5.6$ $F = [0.8,\ 0.8,\ 0.8,\ 0.8,\ 0.6,\ 0.5,\ 0.5]$ $\delta = 0.6$ $\rho = 0.26$	Adaptive control signals for trajectory tracking	Simulation and real-robot experiments Lyapunov-based stability proof	Average error: 4×10^{-3} m
[2]	Interaction force, IMU	12P (5 stroke, 4 spinal cord injury, 3 cerebral injury)	DS: NA DA: private, NA CA: NA	CASIA-ARM	R: RBF neural network	Radial basis function weights updated	Estimation of the subject's motor capability to adaptively regulate assistance and task difficulty in real time	Validation based on task performance and tracking error	Average error: 4×10^{-3} m

In the "Subjects" column, the Healthy (H) and Pathological (P) conditions of the enrolled subjects are reported. In the "Data" column, dataset size (DS), data availability (DA), and code availability (CA) are reported. When this information is not provided, the entry is marked as Not Applicable (NA). In the "Task: Algorithm" column, the task type is specified according to the learning paradigm. For supervised learning, task types include Regression (R) and Classification (C); in the case of classification, the number of classes is indicated in parentheses and followed by the acronym "cl". For reinforcement learning, the task type is specified as Control (Ctrl). In the same column, the name of the algorithm is reported: Radial Basis Function (RBF) neural network, Evolutionary Dynamic Fuzzy Neural Network (EDRFNN), Deep Deterministic Policy Gradient (DDPG), Neural Network (NN) based Actor Critic (AC) learning. In the "Hyperparameters" column, NA indicates Not Applicable.

Table 4. AI Approaches in Robot-Aided Rehabilitation for SA

	Signals	Subjects	Data	Robot	Task: Algorithm	Hyperparameters	Prediction	Validation	Performance
[66]	Postural data	1P (stroke)	DS: 636 trials DA: private, NA CA: NA	Simulated end-effector: Research prototype	Ctrl: POMDP	10 possible actions 82,944 possible states 150 linear value function 150 iterations	Action for the system to execute: setting a new target position and resistance level or stopping the exercise	Online simulations; online application with a therapist and a patient	Agreement: 65.00%
[64, 65]	Pressure, Force, motion data	8P (stroke)	DS: NA DA: private, on reasonable request CA: NA	End-effector: Research prototype	C (4 cl): SVM-RBF	Radial basis kernel function	Compensatory patterns (trunk rotation, trunk lean-forward, shoulder elevation, noncompensation)	LOSO	F1-score: 98.50%
[30]	HR, RR, GSR, T	7H	DS: NA DA: private, NA CA: NA	PUParm robot	C (3 cl): SVM-RBF	Radial basis kernel function	Difficulty level (relax level, medium level, stress level)	LOOCV	Acc: 91.43%
[62]	HR, RR, GSR, T	34H, 17P (stroke)	DS: NA DA: private, NA CA: NA	HapticMaster robot	C (2 cl): Kalman Adaptive LDA	epochs length: 2 min Kalman filtering	Difficulty level (harder and easier difficulty)	LOOCV	Acc: 80.00%
[63]	HR, robot motion	4H	DS: 1,800 data sets (training + test) DA: private, on reasonable request CA: on reasonable request	Exoskeleton: Research prototype	C (3 cl): DNN	Gradient descent optimization Input layer: 10 neurons Hidden layer: 8 neurons Output layer: 4 neurons Activation (Input + Hidden): ReLU Activation (Output): Softmax	Motion intensity to obtain exoskeleton torque (strong, moderate, and weak)	3 subjects for offline test; 1 subject for online test	Acc: 95.70%
[33]	EMG, motion data	10H	DS: 13,000 × 5 DA: private, NA CA: NA	End-effector: Research prototype	R: LSTM-KF	Input dimension: 5 Hidden layer dimension: 64 Data matrix: 13,000 × 5 Sliding window: 200 samples Step size: 10 Back-end layers: 2 FC Dropout layer: Between FC layers Output: 1D predicted perceived torque Batch size: 8 Epochs: 50	Perceived torques	Based on MAE loss	MAE: 0.39

In the "Subjects" column, the Healthy (H) and Pathological (P) conditions of the enrolled subjects are reported. In the "Data" column, Dataset Size (DS), Data Availability (DA), and Code Availability (CA) are reported. When this information is not provided, the entry is marked as Not Applicable (NA). In the "Task: Algorithm" column, the task type is specified according to the learning paradigm. For supervised learning, task types include Regression (R) and Classification (C); in the case of classification, the number of classes is indicated in parentheses and followed by the acronym "cl." For reinforcement learning, the task type is specified as either Control (Ctrl) or Policy Optimization (PO). In the same column, the name of the algorithm is reported: Partially Observable Markov Decision Process (POMDP), Support Vector Machine with Radial Basis Function (SVM-RBF), Kalman Adaptive Linear Discriminant Analysis (LDA), Deep Neural Network (DNN), Long Short Term Memory with Kalman Filter (LSTM-KF). In the "Hyperparameters" column, FC indicates Fully Connected Layer. In the "Validation" column, LOSO Indicates Leave-One-Subject-Out Cross-Validation; LOOCV indicates Leave-One-Out Cross-Validation. In the "Performance" column, Acc indicates Accuracy, and MAE indicates Mean Absolute Error.

The papers are ordered and divided in the aforementioned tables based on the population on which the validation is performed. The scientific contribution gains more and more relevance if the proposed solutions are tested on the target population, i.e., pathological people. This happens in a few cases, while most of the included papers recruit healthy subjects. The last two columns of each table refer to the AI module. In particular, the fourth column classifies whether the faced problem is a C, an R, or an RL one, specifying the number of classes for C problems and detailing the specific ML or DL algorithm. In contrast, the fifth column reports the resulting performance.

In the following subsections, the results of the analyzed papers are presented with a detailed breakdown according to their specific proposed applications, ensuring a clear demonstration of how each result addresses the distinct objectives outlined in the study.

3.1 UIR

UIR plays a pivotal role in personalized and effective robot-aided upper limb rehabilitation. By recognizing the user's intentions, the robot can be controlled accordingly in real-time [34], thereby promoting patient motor outcome, engagement, and motivation throughout the rehabilitation process [35]. User intention is recognized through EMG and IMU sensors, which are placed on the upper limb to identify the movements the user wants to perform. However, motion intention arises from the brain, making it possible to collect EEG data from the scalp and process it to recognize the intended motion. The acquired data can be fed into an AI algorithm that is responsible for detecting and recognizing the user motion intention. By employing these advanced technologies, **Rehabilitation Robots (ReRobots)** can accurately understand user needs and provide tailored assistance, resulting in more effective and successful recovery outcomes for P with impaired arm functions.

In the control framework proposed by Liu et al. [36], a hybrid regression–classification approach is implemented to enhance the responsiveness and stability of human–robot interaction. The regression model, based on Hill's musculoskeletal formulation, estimates the desired joint torque from EMG and joint angle data, enabling continuous torque control aligned with the user's physical effort. In parallel, a **Principal Component Analysis (PCA)** pre-processed data fed into a **Support Vector Machine (SVM)** classifier, which identifies motion versus rest states, stabilizing the robot during static phases and compensating for EMG signal uncertainties. The optimal configuration (400 ms window, 4 PCA components) was integrated into a real-time control loop with an overall delay of about 150 ms, suitable for upper-limb rehabilitation. This hybrid integration, executed in parallel to minimize latency, improves control robustness by suppressing unintended activations.

In [37], a computationally efficient EMG-based motion pattern recognition method is proposed for classifying shoulder-level movements. Raw EMG signals are filtered to remove noise, and features are extracted using a sliding **Root Mean Square (RMS)** with a 540 ms window and 81 ms overlap. For each subject, **Logistic Regression (LR)**, SVM, and **Artificial Neural Network (ANN)** models are trained to perform multi-class classification of four ADLs: arm abduction/adduction, drinking, arm forward/backward, and resting. A one-way ANOVA compared classification accuracies, showing that the SVM achieves superior performance compared to LR and ANN.

In [38], an SVM-based intention recognition framework is proposed to control an upper-limb ReRobot capable of interpreting the patient's motion intentions and delivering the corresponding rehabilitation training. EMG signals from the healthy limb are processed to recognize the intended motion, allowing the ReRobot to assist the affected limb in performing the same movement. Signal pre-processing includes baseline correction, filtering, full-wave rectification, and amplitude normalization to enhance the signal-to-noise ratio. Sample entropy is used for data segmentation, and a Hanning window (128 ms length, 64 ms step) is applied for framing. The system identifies shoulder flexion, abduction, pronation, and elbow flexion as motion intentions, which directly drive the robot's control. Tests on five subjects demonstrate that the SVM-based control achieves high recognition accuracy (F1-score of 93.68%), confirming its suitability for real-time intention-driven rehabilitation.

The study presented in [33] introduces a **Particle Swarm Optimization–based SVM (PSO-SVM)** framework for classifying rehabilitation stages using EMG signals. Here, PSO, an evolutionary algorithm inspired by social behaviors, is employed to optimize SVM hyperparameters, enhancing model accuracy. EMG data were collected during upper-limb flexion and extension tasks performed with the ROKAE Mate ER3 Pro robotic arm. Signals were filtered and segmented to isolate active regions, from which time-domain features were extracted for classification into passive, active, and resistive training stages. During online operation, the trained model generated real-time control and adjustment signals, allowing the robotic arm to adapt the interaction space and control strategy according to the user's motor ability. The proposed system achieved over 93.98% accuracy across all stages. Further discussion of this work appears in Section 3.4, as the work included the application of two AI algorithms used for different functional blocks.

A **Decision Tree (DT)** classifier is employed in [39] to recognize upper-limb movement intentions from EMG signals, supporting the control of a single-lead EMG-based exoskeleton. EMG and joint angle data collected from 10 healthy subjects are processed to extract mean absolute value, RMS, and **Variance (VAR)** features. These features are combined and used to train various classifiers to distinguish between arm flexion and extension. Among the tested algorithms, DT and **Random Forest (RF)** achieved the best performance, with accuracies of 96.36 ± 0.54% and 95.67 ± 0.76%, respectively, outperforming Linear Regression and Polynomial Regression models.

A DT classifier is also applied in [40], achieving 99.00% accuracy in distinguishing pre-intention and intention phases from EMG and motion data. Ten healthy subjects performed three sets of flexion movements, with EMG signals acquired using two surface electrodes and amplified through a g.USBamp system. Signals were sampled at 1.2 kHz and band-pass filtered (5–500 Hz), while joint motion was captured via a potentiometer sampled with a Humsoft MF624. Amplitude-based time-domain features were extracted from each segment, and feature selection was performed using an Extremely Randomized Tree algorithm. A dimensionality reduction approach was tested, but it did not significantly affect performance, confirming the robustness of the full feature set.

Unlike previous studies employing ML algorithms for upper-limb intention recognition, Schabron et al. [41] implement an ANN trained with scaled conjugate gradient **Backpropagation (BP)** to classify 10 distinct hand movements—including various deviations, flexions, extensions, and grasping actions. EMG signals are processed using RMS, median filtering, and mean feature extraction, yielding 24 input features for the ANN. The network architecture comprises 10 hidden layers and achieves a mean classification accuracy of 93.00%. The proposed model demonstrates the feasibility of real-time exoskeleton control during ADLs based on multimovement EMG decoding.

A **BP Neural Network (BPNN)** classifier is introduced in [34] for EMG-based movement detection and exoskeleton control. A 16-dimensional feature space is generated using an autoregressive model followed by PCA, and the resulting features are used as inputs to the neural network to classify shoulder extension/flexion, shoulder abduction/adduction, elbow extension/flexion, and two composite ADLs. The proposed BPNN consists of 3 layers: an input layer with 16 nodes, a hidden layer with 10 nodes, and an output layer with 5 nodes corresponding to the classified arm motions. To further improve performance, a Boosting-based ensemble classification framework is integrated with the BPNN. Tests on two healthy subjects yield a mean accuracy of 95.50%, confirming the effectiveness of the proposed feature extraction and ensemble learning approach in reliably detecting user motion intention.

The work by Guo et al. [42] presents a **Lightweight Convolutional Neural Network (Lw-CNN)** for real-time recognition of upper-limb motion intentions using EMG signals, aimed at robotic arm control during rehabilitation. The network architecture includes two convolutional layers (16 filters, (3×3), stride 1) followed by an additional convolutional layer (32 filters, (3×3), stride 1). Each convolution is followed by a MaxPooling operation ((2×2) kernel) to reduce parameters and prevent overfitting. **Rectified Linear Units (ReLU)** activations, Batch Normalization, and a Softmax output are employed for classification. EMG signals from biceps, triceps, and anterior deltoids were recorded via a 3-channel custom acquisition system featuring an analog front-end with 1,000× amplification and 30–400 Hz band-pass filtering. Data were sampled at 20 kHz, downsampled to 1 kHz, and further processed with a 50 Hz notch filter, 20–450 Hz band-pass filter, and amplitude normalization. Signals were segmented into 192 ms windows with 15 ms overlap, maintaining a total processing delay under 300 ms for real-time operation. The proposed Lw-CNN accurately classifies six upper-limb movements (elbow/shoulder flexion and extension, and their combined motions) with an average Accuracy of 88.75%, outperforming the SVM baseline. Validation on a commercial robotic arm confirms the feasibility of the model for intention-driven rehabilitation control, enabling real-time robotic assistance of the impaired limb.

Differently from previous studies that focused exclusively on healthy subjects, the study by McDonald et al. [43] involved both 10 healthy participants and 4 patients with spinal cord injury to evaluate a myoelectric control strategy for the MAHI Exo-II rehabilitation exoskeleton. The system is designed to activate when muscle activity exceeds a predefined threshold, supporting six control modes: four single-**Degree-of-Freedom (DoF)** setups for two-class problems, and two multi-DoF configurations for four-class problems. For each mode, a **Linear Discriminant Analysis (LDA)** classifier is trained to predict the intended movement direction based on EMG signals acquired during isometric contractions toward virtual targets. Myoelectric signals were recorded from eight muscles associated with elbow, forearm, and wrist movements using the Delsys Bagnoli EMG system. Data acquisition included analog band-pass filtering at 20–450 Hz, sampling at 1 kHz, and digital 4th-order Butterworth filtering in the same range, with mean removal and no additional pre-processing. Features were extracted from 200 ms windows at contraction onset and normalized by the channel-wise average. Classification performance reached 85.00–95.00% Accuracy for single-DoF modes in both healthy and patient groups, while multi-DoF modes achieved approximately 90.00% for healthy subjects and 60.00% for patients. These results highlight the potential of EMG-based exoskeleton control for real-time rehabilitation, particularly in simpler single-DoF applications.

While most previous studies relied on EMG signals for user intention detection, the study by Hernández Antelis [44] employed EEG signals, commonly used in Brain–Machine Interface applications, to recognize movement intentions for robotic assistance. EEG data were acquired during interaction with the Tee-R robot to classify self-initiated and self-selected upper-limb movements, including forearm supination/pronation, arm flexion/extension, and rest. Signal pre-processing involved low-pass filtering at 50 Hz using a 2nd-order zero-phase Chebyshev filter, application of a **Common Average Reference (CAR)** filter, and visual artifact rejection. EEG trials were segmented into 15-second intervals between visual cues, and the zero-time reference was aligned with movement onset signals from the Tee-R system. Feature extraction was performed using the multi-class **Common Spatial Pattern (CSP)** algorithm, and a CNN was trained for classification. The proposed method achieved an average Accuracy of (68.00 ± 15.00%), demonstrating the feasibility of EEG-based intention detection for robotic-assisted movement control.

A DL-based decoding framework to interpret intuitive motor imagery for 3D multi-directional arm movements (left, right, forward, backward, up, and down) using EEG signals is introduced in [45]. The proposed **Multi-Directional CNN, combined with a Bidirectional Long Short-Term Memory (BiLSTM) Network (MDCBN)**, integrates CNN-based spatial feature extraction with temporal sequence modeling. The BiLSTM component includes forward and backward layers with 300 hidden units, and ReLU are applied in the fully connected layer to capture non-linear dependencies. EEG pre-processing involved band-pass filtering (4–40 Hz) using a Hamming-windowed zero-phase FIR filter, Independent Component Analysis for artifact removal, and a CAR spatial filter to improve spatial resolution. Twenty channels near the motor cortices were retained, and data were downsampled from 1,000 Hz to 100 Hz before model input. The MDCBN model, trained with EEG data labeled through kinematic recordings from OPAL sensors, enabled a JACO robotic arm to perform tasks such as reaching and drinking, achieving success rates of (60 ± 14%) and (43 ± 9%), respectively, across 15 healthy subjects. A related approach by Tian [46] employed a **Spatial-Temporal Filtering CNN (STFCN)** to control robotic arm movements in four horizontal directions (forward, backward, left, right) through motor imagery. The STFCN combines multi-class spatial-temporal filtering and convolutional layers with Leaky ReLU activation and dropout rates of 0.2 and 0.3. Tests with six healthy participants demonstrated enhanced decoding performance, reaching (68.10%) Accuracy in offline experiments and (62.70%) in online trials. Although the overall success rates remain moderate, these studies mark the first applications of DL methods for EEG-based robotic arm control.

The use of ML for P300 detection is investigated in [47], where a **Brain–Computer Interface (BCI)** is developed to control a robotic assistant capable of performing 36 upper-limb movements. The system integrates the P300 speller paradigm with a classifier to interpret user intentions. Three algorithms, i.e., SVM, LDA, and Multi-Layer Perceptron, are compared in a two-class setup, where *Target* corresponds to a detected P300 response and *No Target* to its absence. EEG preprocessing includes downsampling, filtering, segmentation into 500 ms epochs, and application of the xDAWN spatial filter to enhance P300-related components. Results from fivefold cross-validation indicate that the SVM classifier outperforms the other tested models. The detected user intention is subsequently translated into a control command to guide the robot's end-effector.

The SVM classifier also proves to be the most effective approach in [48], achieving an average Accuracy of (89.40 ± 5.00%). This study presents a multi-modal architecture for gaze-independent BCI-driven control of a robotic upper-limb exoskeleton, aimed at providing active assistance during reaching tasks in stroke rehabilitation. The BCI interprets the user's motor imagery to determine the intention to initiate or withhold arm movement. EEG data are processed through CSP and band power feature extraction methods before being classified by an SVM. The classifier's output is used to generate kinematic parameters—including speed, acceleration, and jerk—that guide the exoskeleton in real time, ensuring adaptive movement support aligned with the patient's brain activity. Experimental results show that both healthy and stroke participants successfully controlled the exoskeleton, with no significant performance differences observed between the two groups.

3.2 RMP

RMP is a fundamental module of robotic platforms purposely developed for rehabilitation since it is in charge of determining the trajectory to perform a certain motor task, both simple point-to-point and complex movements such as ADLs and/or working gestures.

By combining advanced robotics with intelligent algorithms, motion planning systems can assist in designing tailored rehabilitation programs and in optimizing the therapeutic process. The integration of AI techniques in motion planning further enhances the ability of the system to adapt, personalize, and provide real-time feedback, resulting in improved patient outcomes.

A neuro-fuzzy compensator is introduced in [49] to adapt the dynamics of human–robot interaction and generate real-time trajectories for robotic rehabilitation. The trajectory generation module computes the end-effector positions required to follow a prescribed motion path while simultaneously modulating compliance based on the interaction forces measured at the end-effector. The fuzzy rule base models the relationship between force variations and compliant positional adjustments, enabling smooth and adaptive assistance. By integrating a DL algorithm within the fuzzy compensator, the system autonomously tunes its parameters in real time, enhancing trajectory generation Accuracy and adaptability during rehabilitation exercises.

An enhanced version of the LSTM network, called the **Multi-Stream LSTM Dueling (MS-LSTM Dueling)**, is proposed in [50] to predict multi-joint motion trajectories for the NTUH-II exoskeleton robot. The model integrates both IMU and EMG features to identify motion types and estimate joint angles used for trajectory generation. To enable real-time multi-modal data fusion, IMU and EMG signals are processed in parallel through two specialized branches: an LSTM for kinematic data and a ConvLSTM for muscle activation features. This architecture leverages the linear characteristics of IMU data and the non-linear, spatially correlated nature of EMG signals. The outputs from both branches are combined in a dueling network structure that merges value and stimulation representations to predict joint angles. Pre-processing pipelines are tailored for each modality. IMU data are filtered with a complementary filter to reduce noise, followed by joint angle compensation to correct artifacts from muscle deformation and sensor misplacement. EMG signals undergo notch and high-pass filtering, full-wave rectification, and moving average smoothing, with additional time–frequency analysis via Short-Time Fourier Transform using a Hamming window to produce a (10×16) feature matrix per sample. Temporal synchronization between IMU and EMG data is achieved by aligning signals within time windows corresponding to the lower sampling frequency. The predicted joint angles are fed in real time to the exoskeleton's PID controller, enhancing human–robot coordination by minimizing delay. Experimental results show that the MS-LSTM Dueling model achieves higher prediction Accuracy and lower latency compared to other state-of-the-art approaches.

A hybrid LSTM-CNN model is presented in [51] for path planning of upper-limb movements during two daily tasks: drinking water and touching the head. The algorithm takes as input joint angle data recorded by a motion capture system and predicts the corresponding elbow and wrist angles, establishing the relationship between the shoulder and elbow joints to generate the full upper-limb trajectory. In parallel, human active interaction is incorporated through an impedance/admittance model that refines the trajectory in real time. The network architecture includes two convolutional layers, two pooling layers, two dropout layers, two LSTM layers, and two fully connected layers with ReLU activation functions. Compared to the BP model, the proposed LSTM-CNN achieved higher (R^2) values, demonstrating improved adaptability of the generated trajectories to different patients.

A BPNN is developed in [1] to predict the elbow joint angle of the healthy upper limb within an intention-based bilateral training system using a cable-driven **Powered Variable Stiffness Exoskeleton Device (PVSED)**. The system enables real-time motor rehabilitation by estimating the intended movement of the intact limb from EMG signals and transferring it to guide the impaired limb. Raw EMG data are processed with a 50 Hz notch filter and a 4th-order Butterworth band-pass filter. To address inter-subject variability, signal normalization is performed using the isometric maximal voluntary contraction method. The elbow joint angle of the intact limb, measured via an IMU, serves as the ground truth for supervised learning. The BPNN consists of an input layer, a hidden layer, and an output layer, trained offline using a multi-feature vector comprising nine time- and frequency-domain EMG features. The network's output is used for online myoelectric control, where the predicted trajectory drives the exoskeleton through a low-pass filter and a PID controller. Among the tested input configurations, the multi-feature vector achieved the best performance, with a correlation coefficient of 90% and an RMSE of 21∘, demonstrating accurate and consistent prediction of joint motion for rehabilitation applications.

A comparable approach is presented in [52], where an EMG-driven bilateral training system using an exoskeleton is developed to mirror the movements of the unaffected limb onto the affected one. The method employs a CNN-LSTM architecture that integrates both EMG and motion data collected from 10 healthy participants. Raw EMG signals, recorded at 200 Hz from eight Myo armband channels, were pre-processed using a 20 Hz high-pass filter to remove low-frequency noise and a built-in 50 Hz notch filter to eliminate power line interference. IMU data, sampled at 20 Hz, underwent pre-processing through an embedded Kalman filter for denoising and smoothing. To synchronize the modalities, a sliding window segmentation was applied: EMG data were divided into 250 ms windows (50 samples) with 50 ms increments, while IMU data were segmented into 25 ms windows with 5 ms increments. Each EMG window was reshaped into a (50×8) image as model input. The CNN-LSTM network includes one convolutional layer, two LSTM layers, two fully connected layers, and a regression output layer, and is designed to predict continuous elbow flexion–extension motion. The proposed system achieved high Accuracy in both offline and online tests, reporting a correlation coefficient R^2 of 0.93, demonstrating robust and precise bilateral motion estimation for exoskeleton-assisted rehabilitation.

The use of **Hidden Markov Models (HMM)** for developing a **Learning by Demonstration (LbD)** path-planning method is explored in [53]. Specifically, the HMM Bakis Left–Right algorithm is employed to analyze therapist demonstrations and identify the most representative trajectory, defined as the one with the highest probability. The experimental setup involved five therapists and one healthy participant, each performing five demonstrations of a specific movement consisting of four joint-space trajectories executed in passive mode. The resulting sequences of joint states served as inputs to the HMM. To ensure physiological plausibility, a joint synchronization step verifies the proper activation order of joints, typically following a proximal-to-distal pattern (e.g., shoulder preceding elbow). Movement onset is detected when joint velocity exceeds 5% of its maximum, and average inter-joint time differences across demonstrations are used to align trajectories temporally, preserving human-like coordination. In the second experimental phase, the learned trajectories were executed online and compared with state-of-the-art methods using kinematic and human-likeness indicators, along with therapist evaluations. The system achieved an agreement rate of 70.40%, with therapists confirming that the generated movements accurately reflected their intended trajectories and were appropriate for rehabilitation exercises.

A related imitation learning approach based on **Probabilistic Movement Primitives (ProMP)** is presented in [54]. This probabilistic framework models the distribution of motion data to align the ReRobot's trajectories with the user's natural movement patterns. The proposed method employs five **Radial Basis Function (RBF)** activation functions to encode motion variability and ensure smooth trajectory generation. Compared to the traditional **Dynamic Movement Primitives (DMP)** algorithm, the ProMP-based approach achieved lower trajectory jerk and reduced variations in position, velocity, and acceleration parameters, demonstrating an improved ability to generate human-like training trajectories for rehabilitation.

A **Deep RL (DRL)** algorithm for robot trajectory planning is proposed in [55], aiming to enable obstacle avoidance and accurate target reaching. The model introduces two dense reward functions, termed *azimuth* and *aspiration* rewards. The azimuth reward constrains exploration within a reasonable range, while the aspiration reward encourages the agent to explore unfamiliar environments. The latter incorporates a feature extractor and a Recurrent Neural Network with Hierarchical Memory (SRU-HM) to enhance long-term decision-making. The DRL model receives normalized state information and the agent's actions as inputs, and outputs the predicted next state. Simulated experiments involving one and two obstacle scenarios integrate the proposed reward functions into **Asynchronous Advantage Actor-Critic (A3C)** and **Distributed Proximal Policy Optimization (DPPO)** algorithms. Results show that combining both reward functions improves convergence speed and trajectory planning quality compared to using either reward alone. Among the tested methods, DPPO achieved the highest reward of 1,970.60 when avoiding two obstacles, converging in 258 episodes, while A3C reached a reward of 1,968.40 in 296 episodes, confirming the superior efficiency of the DPPO-based framework.

3.3 RIC

Robot control refers to the process of governing the physical movements and actions of a robot. It involves generating and executing commands or control signals to manipulate the robot actuators, such as motors or servos, to achieve desired motions and behaviors.

Learning-based control techniques have gained prominence in robot control. These methods leverage data-driven models and algorithms to learn control policies from experience or training data. AI enables robots to adapt, optimize, and generalize their control strategies based on specific tasks or environments along with changing conditions [56].

With the aim of developing a bilateral collaborative rehabilitation training robot, Xiao et al. [29] propose an adaptive **Proportional–Integral–Derivative (PID)** controller enhanced by an RBF neural network. The control architecture acquires motion data from both the healthy and affected limbs, generating robot commands based on their movement difference to facilitate coordinated rehabilitation training. This setup enables the execution of elbow flexion and wrist rotation tasks while promoting symmetric movement patterns. The proposed model was validated through simulation rather than experimental trials with participants. Although no quantitative performance metrics are reported, the simulation results compare the standard PID and RBF-PID controllers, showing that the latter achieves accurate motion tracking with an angular error of $\leq$0.09 rad. These findings suggest the potential of the RBF-PID system to support game-based mirror therapy rehabilitation.

A simulated environment is also employed in [57] to evaluate an adaptive impedance controller based on an **Evolutionary Dynamic Fuzzy Neural Network (EDRFNN)**. The controller takes as inputs the mechanical impedance parameters of the impaired limb and the desired impedance control parameters, producing adaptive outputs for real-time control. The EDRFNN architecture consists of an input layer, a membership layer, a rule layer, a normalization layer, and an output layer. The key idea behind this controller is to allow the robot to dynamically adjust the desired impedance according to the user's current recovery condition. The impairment level is estimated by identifying the damping and stiffness parameters of the affected limb using a **Slide Average Least Squares (SALS)** algorithm. Offline optimization of the network parameters is performed through **Genetic Algorithm (GA)** and **Hybrid Evolutionary Programming (HEP)**, while a dynamic BP learning algorithm provides online adaptation based on error gradient descent. The controller is tested in a Matlab-simulated 2-DoF ReRobot, using impedance parameters derived from previous studies as the initial conditions for the SALS identification. Comparisons with models lacking GA, HEP, or BP optimization show that the EDRFNN achieves superior results in both time regulation and position tracking Accuracy. Overall, simulation outcomes confirm the robustness and adaptability of the proposed controller, highlighting its potential for real-world rehabilitation and assistive robotic applications.

An **Actor–Critic (AC)**-based DRL controller is presented in [58] to develop an autonomous framework for intelligent robot-assisted therapy, where the system automatically tunes the parameters of a PID controller. The approach, implemented on the iTbot ReRobot, uses a **Deep Deterministic Policy Gradient (DDPG)** network to adjust the controller gains and generate smooth joint torques for accurate trajectory tracking, minimizing the need for human supervision during therapy. The agent receives environmental observations, including joint angles, velocities, tracking error, and its derivative and integral, and outputs the corresponding PID tuning parameters. The reward function is designed based on tracking error, torque effort, and a boundary constraint indicator for joint space limits. This formulation enables the agent to efficiently converge toward the optimal control policy. Simulation results demonstrate precise motion tracking, achieving a maximum tracking error of 0.16 rad, confirming the effectiveness of the proposed DRL-based adaptive control strategy for rehabilitation applications.

A combined simulation and experimental validation on healthy subjects is presented in [59], where an adaptive inverse optimal hybrid control strategy integrating inverse optimal control with a neural network–based AC learning framework is proposed. The model is first evaluated in simulation and subsequently tested on five healthy participants to assess its feasibility in a rehabilitation context. Comparative analyses show that the proposed controller outperforms traditional approaches in terms of position tracking Accuracy, position error, and control torque. Specifically, it achieves a position error of 0.05 rad, which is lower than the value reported in [29]. These results demonstrate that the NN-adaptive inverse optimal hybrid controller can effectively evaluate user performance and autonomously adjust its assistance or resistance level to match the patient's rehabilitation needs.

In contrast to previous studies conducted solely on healthy participants, the models in [2, 60] were validated on a pathological population. In particular, Luo et al. [2] introduce an **Assist-As-Needed (AAN)** controller enhanced with RBF networks. The AAN framework aims to deliver optimal robotic assistance that supports task completion while motivating patients to contribute actively to the movement. By integrating a greedy strategy with the AAN controller (GAAN) and RBF networks, the system adaptively tunes assistance levels based on the patient's motor capability and performance to minimize tracking error. Kinematic and dynamic data were collected at 1,000 Hz, and the RBF network weight vectors were continuously updated according to each patient's state and performance metrics. Experimental results with 12 patients demonstrated average tracking errors on the order of (4×10^{-3}) m under various conditions, including left-to-right and right-to-left movements, and across different assistance levels (no-RBF, low-RBF, and high-RBF). These findings confirm the effectiveness of the GAAN–RBF approach in providing adaptive, patient-specific robotic assistance during rehabilitation.

A **Neural-Fuzzy Adaptive Controller (NFAC)** based on a **RBF Network (RBFN)** is presented and validated in [60] on one healthy subject and two stroke patients. The adaptive controller is implemented on an upper-limb exoskeleton designed to support passive rehabilitation training involving shoulder flexion/extension, elbow flexion/extension, and wrist ulnar/radial deviation. The neural network compensates for non-linearities in the human–robot interaction, taking joint position, velocity, and acceleration vectors as inputs and producing an adaptive control term as output. This term enables the exoskeleton to apply assistive forces according to feedback from force/torque sensors. Two experimental protocols, trajectory tracking and frequency response, are conducted to evaluate the controller's performance. The results are compared with those of a **Cascaded PID (CPID)** controller and a **Fuzzy Sliding Mode Controller (FSMC)**. The proposed RBFN-based NFAC achieves lower position tracking error and superior frequency response characteristics, with an average RMSE of 0.03 rad for shoulder flexion/extension, compared to 0.06 rad and 0.04 rad obtained with CPID and FSMC, respectively. These outcomes confirm the effectiveness of the adaptive control approach in improving motion Accuracy and stability during rehabilitation tasks.

3.4 SA

Robots can utilize sensors to monitor users' physiological signals, such as HR, RR, GSR, and T, to estimate their emotional states. User state estimation can help the robot in adapting its behavior to provide appropriate assistance or feedback. For this reason, the SA module plays a crucial role in enhancing the physical interaction between humans and robots because robots can tailor their responses, provide personalized assistance, and create more engaging and effective HRI depending on a user's condition, behavior, or intent [61].

The approach presented in [30] applies a classification-based method to adaptively and dynamically adjust rehabilitation therapy according to each patient's physiological state. The system uses HR, RR, **Skin Conductance Level (SCL)**, **Skin Conductance Response (SCR)**, and temperature (T) as input features to predict the appropriate difficulty level of a VR training game. Physiological signals are sampled at 2.4 kHz using a g.USBamp amplifier (g.tec medical engineering GmbH) and processed through a multi-modal pre-processing pipeline. HR, RR, and T are normalized by baseline subtraction and division, while SCL and SCR are normalized by baseline subtraction only to account for their zero-referenced nature. This ensures inter-subject comparability and improves signal robustness. Subsequently, PCA is applied to the normalized data to perform feature reduction and retain the most informative components. Nine AI algorithms are evaluated using LOOCV, with the SVM employing an RBF kernel achieving the highest Accuracy of 91.43%. The selected model is then used for real-time validation, where the difficulty level of the game is updated every 30 seconds: it decreases when the user is overstressed, increases when relaxed, and remains constant otherwise. This adaptive mechanism enables short-term, real-time adjustment of therapy intensity while maintaining stable and user-tailored interaction dynamics.

The study in [62] introduces a biocooperative feedback loop for upper-limb rehabilitation that adaptively adjusts task difficulty based on a fusion of task performance, biomechanical data, and physiological signals such as HR, RR, SCL, SCR, and temperature (T). The rehabilitation task involves reaching and grasping actions within a virtual environment, where participants catch a ball and place it into a basket, supported by haptic feedback that reproduces interaction forces with virtual objects. The system adapts the difficulty level every 2 minutes, allowing the controller to respond to short-term changes in the user's state while preserving overall stability. Each signal modality is pre-processed within fixed 2-minute time windows, extracting and normalizing features such as HR variability, skin conductance, and movement metrics. All signals are synchronized using a common timing reference and combined through LDA for binary classification (increase or decrease difficulty). To manage inter-subject variability and enable online learning, a Kalman Adaptive LDA is implemented, updating the discriminant function after each task window based on user-specific feedback. The experimental population includes 34 healthy participants and 17 hemiparetic patients. Results show that psychophysiological signals alone have limited predictive power but significantly improve performance when combined with biomechanical and task-related data. The Kalman Adaptive LDA achieves classification accuracies of 84.7% for healthy subjects and 89.4% for patients, i.e., approximately 10% higher than when using physiological features alone, demonstrating the benefit of multi-modal data fusion for adaptive rehabilitation control.

The study presented in [63] employs a multi-modal approach that integrates the physiological state and robot motion signals to assess and adapt rehabilitation training intensity, with the patient's condition represented solely by HR. Kinematic acceleration data are collected from both the encoder integrated into a disc motor and another placed on the rear of a stepper motor. These measurements are used to compute joint relative velocity differences, representing the mismatch between the motion intensity of the exoskeleton and that of the user. To enhance robustness and mitigate errors caused by abrupt accelerations or decelerations, pre-processing involves collecting angle data from the first 3 seconds of each movement phase and calculating the average difference between the actual and reference joint trajectories. HR and motion features are standardized using Z-score normalization to balance scale and VAR differences, improving training stability. The resulting multi-modal feature vector, consisting of six eigenvalues from HR and motion data, is fed into a **Deep Neural Network (DNN)** with three layers (10 neurons in the input layer, 8 in the hidden layer, and 4 in the output). The network employs ReLU activation for the first two layers and Softmax in the output to classify motion intensity into three categories: strong, moderate, and weak. Comparative evaluations demonstrate that the DNN achieves superior performance, with an average motion intensity recognition Accuracy of 95.7% on the test dataset. The online estimation of motion intensity enables real-time adaptation of rehabilitation training, allowing for personalized therapy tailored to each user's physical condition.

Unlike previous studies that relied on physiological signals for SA, the works in [64, 65] utilize pressure, force, and motion data from eight stroke patients to classify compensatory movement patterns using an SVM with an RBF kernel. The proposed pressure distribution-based compensation detection system records pressure data while participants perform three reaching tasks, enabling the identification of maladaptive motor behaviors during rehabilitation. Each pressure map is represented as a (32×32) vector, from which 10 descriptive features are extracted, including average and maximum sensor values, average, and standard deviation of medial/lateral and anterior/posterior centers of pressure, and pressure ratios in both directions. These features capture spatial and statistical characteristics of the pressure distribution and are standardized to ensure inter-subject and inter-session comparability before being fed into the classifier. The SVM-RBF model achieves an F1-score of 98.50% in the online detection of compensatory patterns. Once compensation is identified, a force feedback mechanism is triggered through the ReRobot to suppress undesired movements, thereby promoting correct motor execution during therapy.

In a RL framework, Kan et al. [66] employ a DRL algorithm to adapt robotic behavior based on patients' postural data during upper-limb rehabilitation. The system is modeled using a **Partially Observable Markov Decision Process (POMDP)** to autonomously guide reaching exercises for moderate stroke patients, personalize training parameters, and estimate user fatigue in real time. The study involves one therapist and one right-sided hemiparetic patient, complemented by several simulation trials. Following an initial offline training phase, the DRL controller's decisions are compared with those of a human therapist to evaluate its clinical reliability. The therapist's feedback indicates a 65% agreement with the AI system's decisions, suggesting that the proposed POMDP-based adaptive framework can approximate expert reasoning while autonomously adjusting rehabilitation parameters to the patient's state.

Another approach for SA is proposed in [33], where EMG and motion data are combined to predict the perceived torque and adjust the assistance gain in an AAN control scheme. The signals, collected under seven experimental conditions from 10 healthy participants, are processed using a **Long Short-Term Memory network with a Kalman Filter (LSTM-KF)** R model to quantify the assistance level provided by the ROKAE Mate ER3 Pro robotic arm based on user engagement during rehabilitation. Before training, EMG signals undergo a fifth-order Butterworth band-pass filter to remove low-frequency noise from power line interference, electrode movement, and motion artifacts. Only channels from the biceps and triceps brachii are retained, and a thresholding strategy is applied to keep the top 70% of signal amplitudes, discarding inactive segments. The model input consists of a fused five-dimensional vector including two EMG channels and three kinematic features (joint angle, first- and second-order differences). The LSTM-KF network comprises an input layer, an LSTM-KF block with 64 hidden units, a fully connected layer with dropout, and an output layer, trained for 50 epochs with a batch size of 8. The model outputs a continuous value representing the predicted perceived torque, which is used to adapt the robot's control parameters in real time. Evaluation based on the MAE yields values of 0.39, confirming the effectiveness of the LSTM-KF model in estimating perceived torque and supporting online adjustment of assistance levels in clinical rehabilitation scenarios.

4 Discussions

The findings from this systematic review highlight the utility of AI in various aspects of upper limb rehabilitation, encompassing UIR, RMP, RIC, and SA.

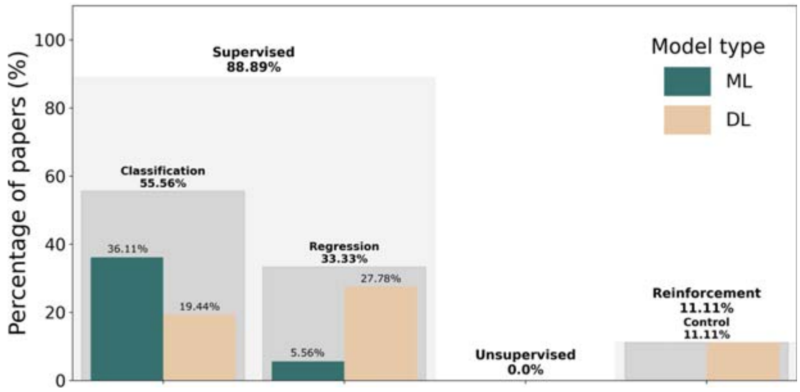

Fig. 3. Bar plot representing the distribution of AI approaches used in the included studies, categorized according to the learning paradigm within the "Algorithm" thematic area. The paradigms include Supervised, Unsupervised, and RL. For Supervised Learning (highlighted by the light gray shaded area), the plot further distinguishes task types into Classification (C) and Regression (R), with the corresponding percentages indicated using additional darker shading. Each task type is also broken down by model type: ML or DL, as shown by the color-coded bars. No studies based on Unsupervised Learning were found. RL is presented separately and also subdivided by model type (ML or DL). The color legend helps differentiate between ML and DL model types, supporting the interpretation of their distribution across task types and learning paradigms.

To address research question *Q2*, which concerns the examination of data-driven learning methodologies applied to specific tasks within the identified modules, a bar chart was created to illustrate the distribution of approaches across the reviewed studies. As shown in Figure 3, the plot summarizes how different ML paradigms, i.e., Supervised, Unsupervised, and RL, are represented in the reviewed literature. Within Supervised Learning, tasks are further categorized as C and R, each analyzed separately for traditional ML and DL models. The shaded areas highlight the overall contribution of each learning type and its subcategories, while the color-coded legend distinguishes ML and DL approaches, providing a clear visual overview of the methodologies used across different task types.

The chart clearly shows that none of the papers included in this review adopt unsupervised learning approaches. Supervised learning emerges as the most commonly employed paradigm, with C problems being the most frequently addressed, predominantly using ML algorithms. In contrast, R problems are less commonly tackled with ML models, and no ML approaches are applied in RL contexts.

Moreover, it is worth observing that 41.17% of included works are about UIR, 22.22% are about RMP, 16.67% are about RIC, and 19.44% are about SA. So, most of the papers have UIR as their AI-driven module, and this could be the reason why C has achieved the highest percentage of occurrences, as shown in Figure 3 (bar). Among both C, R, and RL methods, the most recurrent algorithms belong to DL. In fact, the adoption of DL algorithms has emerged as a dominant trend in the field, and its prevalence surpasses other ML approaches and traditional methods. This can be attributed to several factors, including the ability of DL models to automatically extract relevant features from the data, reducing the need for manual feature engineering [67]. Additionally, the capacity of DL models to handle large datasets enables improved classification performance [68]. At the same time, the non-linear activation function integrated into the proposed DL algorithms represents a useful tool in treating a non-linear relationship established between robot and patient [60]. More specifically, most of the applied DL algorithms have in common:

- the deep neural structure;
- the BP learning method via the gradient descent algorithm;
- a specific architecture for each problem;
- a non-linear activation function.

Furthermore, to summarize the data-driven learning methodologies applied within the analyzed functional modules, the individual percentages for each AI-driven module are reported below:

(1) UIR: 100.00% C, of which 60.00% ML and 40.00% DL;
(2) RMP: 87.50% R, of which 25.00% ML and 62.50% DL; 12.50% RL with DL;
(3) RIC: 66.67% R with DL and 33.33% RL with DL;
(4) SA: 71.43% C, of which 57.14% ML and 14.29% DL, 14.29% R with DL, 14.29% RL with DL.

In UIR, the dominance of classification techniques, supported by a blend of ML and DL, highlights the significance of accurately deciphering user intentions for effective upper limb rehabilitation. However, it can be seen from Table 1 that most performance values obtained are above 80%. This is obtained especially for the most recurrent ML algorithm, i.e., SVM, that achieves high-performance value in every classification problem. Indeed, for the application of DL algorithms, there is no unique network used, but they all are designed and adapted to the specific case and dataset.

Nevertheless, even in the application of DL algorithms, Accuracy scores higher than 88% are found except for the detection of user intention from brain activity [44–46]. In fact, the difficulty in processing and deciphering the EEG signals resulted in lower performance values than the other works included in this category. However, the novelty introduced in [44–46] lies in the fact that for the first time a DL algorithm was applied to solve UIR problems using EEG, so it lays the foundation for future use of DL algorithms in this context.

It emerged from the aforementioned analysis that classification models excel in discerning discrete user actions, even with the application of very simple models such as SVM.

Lastly, the absence of R instances could be attributed to the inherent nature of intention recognition as a classification task. Despite the use of classification algorithms for all papers included in the UIR category, it is difficult to make a detailed comparison of the algorithms used and performance obtained because each application and result depends on the dataset used, thus, the number of subjects involved, the type of task performed, and the number of classes for the classification problem.

In the specific context of RMP and RIC, treating R problems with DL algorithms has demonstrated a greater efficacy. The models capability to comprehend intricate robot and human–robot system dynamics has led to more fluid and efficient motion outcomes. At the same time, the highest utilization of R, particularly through DL, in both RMP and RIC indicates the efficacy of continuous output prediction for smooth robot movements. Simultaneously, the inherent adaptability of DL models aligns well with the dynamic nature of real-time control scenarios. These features have substantial implications for optimizing the execution of rehabilitation exercises and enhancing patient outcomes. In particular, the most used models are neural networks applied to regressive problems, so the performance is expressed in terms of errors and correlations, as it can be seen in Tables 2 and 3. Both correlation and error values demonstrate the capability of the proposed AI methodologies to accurately perform both motion planning and robot control tasks. In fact, correlation coefficients are higher than 90%, while error values are lower than 1, reaching the best result of 4×10^{-3} m in [2, 60].

However, each study included in this review has focused attention on different models: for RMP, for example, the only model that has been applied in more than one paper is the LSTM-CNN, which effectively captures both spatial features and temporal dynamics to enhance the model's ability to predict and navigate complex, time-varying environments; whereas for RIC, the only model used in more than one paper is the RBF neural network. This network offers advantages such as adaptability to non-linear functions, good generalization, quick learning during training, and interpretability. However, it has some limitations, including the need for substantial training data, difficulty adapting to dynamic changes, challenges in parameter determination, and computational costs. The effectiveness of RBF networks in robot control depends on specific contexts, problem characteristics, and DA [69]. Similarly, the LSTM-CNN model, despite its strengths, also has limitations such as high computational demands, complexity in hyperparameter tuning, and the need for extensive training data. The effectiveness of LSTM-CNN in RMP is context-dependent and requires careful consideration of problem specifics and available resources. Additionally, these dependencies also influence the choice of model to be adopted for different purposes: public datasets might be helpful in order to ensure a comparison of the various regression models. Moreover, the majority of RL problems are treated in these fields. DRL is significantly advancing both RMP and RIC, providing robots with the capability to learn from the users' movements and adapt their strategies to individual needs based on real-time feedback. These robots can develop precise motion plans that guide the patient's arm through therapeutic exercises, ensuring that movements are both safe and effective. However, each included works has introduced a different RL model based on the problem specifications.

Conversely, in the context of SA, predominant attention is given to the utilization of C models. In fact, the work in [66] applies an RL approach to adapt the robot behavior both in a simulated environment and on a stroke patient. For [66], usual performance is not reported in Table 4: in fact, the results obtained are expressed in terms of agreement, that is, the therapist agreed with the robot's actions and choices during rehabilitative physical therapy in 65% of the actions. A similar approach was used also in RMP [53], where an agreement of 70.40% was reached for the development of an LbD system (see Table 2). Additionally, a regression has been applied by [33] to provide real-time the appropriate torque, and so the assistance level, according to the EMG recordings. For the other four works included in the SA category, an Accuracy value above 80% is achieved for both the application of ML and DL algorithms. However, only the SVM-RBF has been used in more than one case [30, 64, 65], otherwise each work included in this category has a different algorithm applied. The inclusion of SVM-RBF suggests an awareness of handling non-linear data patterns efficiently. Additionally, the utilization of Kalman Adaptive LDA underscores the importance of dynamic adaptability to changing data conditions, a crucial aspect in SA scenarios. Furthermore, the incorporation of DNN indicates a recognition of the ability to capture intricate and abstract data representations.

The awareness of model complexity is evident due to the inclusion of SVM-RBF, Kalman Adaptive LDA, and DNN, algorithms that provide a comprehensive toolkit for addressing various data characteristics and adaptation challenges. These models strike a balance between performance optimization and the practical management of complexity. Moreover, the inherent tradeoff between model complexity and interpretability is acknowledged. While SVM and Kalman Adaptive LDA offer simplicity and interpretability, the inclusion of DNN raises computational resource issues. But, similarly to UIR, it is difficult to compare the performance obtained because the datasets used in the various research works are different. Additionally, the emphasis on classification methodologies underscores the essential flexibility intrinsic to effective SA. The aptitude of classification approaches for decision-making tailored to specific user states is further amplified through the enriched pattern recognition and learning capabilities contributed by DL and ML. Specifically, C models, especially when reinforced by ML and DL techniques, possess the capacity to dynamically make adaptive

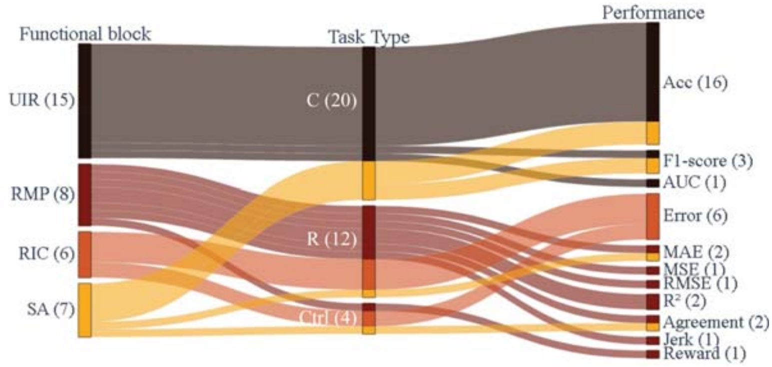

Fig. 4. Parallel categories diagram showing how different functional blocks (UIR, RMP, RIC, SA) relate to the task types and reported performance metrics across the analyzed studies. Color encodes the functional block, and tick labels include the number of studies per category. Acc, Accuracy; AUC, Area Under Curve; C, Classification; MAE, Mean Absolute Error; MSE, Mean Square Error; R, Regression; RIC, Robot Interaction Control; RMP, Robot Motion Planning; RL, Reinforcement Learning; RMSE, Root Mean Square Error; R^2, coefficient of determination; SA, System Adaptation; UIR, User Intention Recognition.

decisions grounded in real-time user data. This adaptive responsiveness assumes paramount significance in promptly tailoring the rehabilitation protocol to seamlessly accommodate changes in user capabilities. Consequently, this adaptive framework significantly enhances the overall efficacy of the intervention, fostering a more optimized and personalized rehabilitation experience.

While the bar chart addresses *Q2* by providing a quantitative overview of the algorithmic approaches identified in the literature, the parallel categories diagram in Figure 4 was developed to respond to *Q3*, which concerns the analysis of performance metrics and evaluation strategies used to assess the effectiveness of AI methods, with attention to their consistency across studies. This visualization enables a multi-dimensional representation of the relationships between functional modules (UIR, RMP, RIC, SA), task types, and performance measures, thus offering a comprehensive view of how evaluation strategies are distributed across the reviewed works. In the "Performance" column, all error-related metrics (e.g., position error, tracking error) are grouped under the macro-category named "Error." When multiple performance measures were reported within a single study, the most representative and relevant one was selected for inclusion. The parallel categories diagram is particularly suitable for addressing *Q3*, as it allows simultaneous visualization of how different methodological dimensions interact, revealing trends and inconsistencies in evaluation practices. At the same time, it highlights a major limitation of the current literature, i.e., the lack of standardized performance metrics, which hinders direct comparison across studies. The heterogeneity in research goals, data types, and implementation details within each functional module makes it difficult to apply a consistent evaluation framework. As a result, studies often rely on distinct performance metrics that are selected based on the specific context in which the AI model is used. For instance, even when addressing similar tasks, such as classification within modules like RMP or SA, researchers report a wide range of metrics, including Accuracy, F1-score, AUC, and error-based indicators, often without a shared benchmark or reference dataset. This fragmentation prevents a fair comparison of model performance and hinders a unified understanding of the strengths and limitations of different approaches.

This variation is not only observed across different functional blocks but also within them, making it challenging to assess the relative effectiveness of algorithms or approaches in a unified manner. The presence of both regression- and classification-based metrics within similar contexts further exacerbates this issue. Consequently, no quantitative meta-analysis or ranking of model performance was possible, limiting the generalizability and comparative interpretability of the findings.

In conclusion, the observed distribution of AI methodologies across upper limb rehabilitation reflects their suitability for the specific functional modules identified (*Q1*) and the tasks addressed within them. For instance, in modules such as UIR and SA, the choice between ML and DL depends on factors including DA, computational resources, and the complexity of the task. ML approaches are generally more interpretable, require less data, and are computationally less demanding, yet they may struggle with complex relationships. DL approaches, in contrast, can automatically learn intricate features from large and complex datasets but require substantial data and computational power. Consequently, it is not possible to determine *a priori* the best algorithm for a given context, as the optimal choice is strongly influenced by dataset characteristics, task requirements, and the study's objectives (*Q2*). Furthermore, the analysis of performance metrics and evaluation strategies (*Q3*) reveals considerable heterogeneity across studies, highlighting the need for standardized datasets and benchmarking procedures. The availability of public datasets could facilitate the application of different algorithms and enable more consistent and meaningful comparisons of performance across studies.

4.1 Opportunities and Future Direction

This literature review has facilitated the integration of contemporary research findings about integrating AI methodologies within the functional building blocks of robot-aided rehabilitation architectures. Furthermore, this systematic approach has enabled the identification of potential challenges and future research directions that could be pursued to enhance the effectiveness and reliability of these systems such as:

(1) Exploring the use of multi-modal monitoring and learning: the review indicates a limited consideration of physiological parameters beyond EMG. Integrating additional signals, such as HR, RR, GSR, T, and EEG, can offer a more comprehensive representation of the patient's physical and cognitive condition [70, 71]. This need for integrating additional physiological signals is underscored by situations where EMG data may be unavailable due to neuromusculoskeletal conditions such as spasticity, paralysis, muscle damage, or nerve damage. These conditions can result in unintended muscle contractions and forces, making EMG and interaction force data less reliable for accurately assessing patient movement or intention. This underscores the importance of exploring solutions that leverage multi-modal monitoring systems to comprehensively describe patients' states during physical interactions with ReRobots. Moreover, the multi-modality of the collected data presents a significant challenge in developing intelligent processing systems that can effectively handle information of diverse natures in real-time. With the broadening of the signals to be analyzed and the need for increasingly customized systems, AI methodologies can provide a significant driving force for the integration of precision medicine into operational contexts. Therefore, future research should explore:
   - which additional physiological signals, beyond EMG, could enhance system awareness;
   - how such signals can be effectively incorporated into existing rehabilitation protocols;
   - what design strategies and implementation guidelines are most effective for developing multi-modal monitoring systems in robotic rehabilitation;
   - to what extent multi-modal learning approaches can offer improvements over unimodal ones.

(2) Promoting methodological alignment and standardization in evaluation practices: a critical limitation identified through this review is the lack of consistency in the performance metrics used across the literature. Even within similar functional blocks or treated problem, studies

often report different performance metrics without a common reference framework. This heterogeneity prevents direct comparison of results and limits the generalizability of findings. Future research should therefore address the following issues:
- the definition of guidelines that encourage the adoption of shared evaluation practices within the research community;
- the development of standardized evaluation frameworks to ensure comparability between studies;
- the identification of the most appropriate performance metrics that allow for consistent evaluation across AI-based rehabilitation systems.

(3) Improving transparency and reproducibility through data and CA: a significant limitation observed in the reviewed literature is the frequent lack of access to datasets and source code, as well as missing details regarding the input data used to train and evaluate AI models. This compromises reproducibility, hinders validation by independent researchers, and limits the possibility of fair benchmarking between approaches. Future efforts should be addressed to the research community:
- encourage the research community to enforce the publication of datasets and source code related to AI-driven rehabilitation systems;
- investigate what are the minimal information requirements (e.g., on input signals, preprocessing, or feature extraction) that should be reported to ensure transparency and replicability;
- strengthen the ethical and regulatory framework to make clinical or sensitive rehabilitation data publicly accessible.

(4) Validating the AI methodologies with pathological populations and evaluating their clinical impact: most current studies have limited validation with pathological populations, which is crucial for real-world application. Among the reviewed literature, only a few studies [43, 60, 62] evaluated their models on both H and P populations. However, these studies generally did not investigate clinically meaningful outcomes or use standardized clinical assessments. More critically, the impact of the AI module itself on clinical improvement has not been investigated in the included works. Performance metrics are often reported without clear interpretation in terms of clinical benefit, making it difficult to determine whether the AI contributes meaningfully to patient recovery beyond standard rehabilitation. In rehabilitation settings, where the clinical relevance of technological interventions is paramount, it is essential to go beyond reporting algorithmic performance and demonstrate actual effectiveness in real clinical scenarios. This requires not only the adoption of standardized clinical outcome measures, but also the ability to explicitly link AI-driven decisions to meaningful functional improvements in patients. Establishing this connection is crucial to validate the readiness and real-world applicability of AI-based rehabilitation systems in healthcare practice. Future research should address the following topics:
- the development of protocols and methodologies to enable the transition of AI-driven systems from research to clinical practice;
- the identification of specific clinical outcomes to be prioritized for assessing the effectiveness of AI-driven rehabilitation systems;
- the expansion of clinical validation to include diverse pathological populations and longitudinal studies aimed at evaluating long-term efficacy;
- the methods by which studies can explicitly quantify the clinical contribution of the AI component within rehabilitation systems.

Additionally, transfer learning is emerging in the current literature as a promising strategy for addressing limitations related to DA and generalizability. By adapting models initially trained on healthy populations to pathological cohorts, transfer learning could accelerate clinical translation, improve model robustness, and enable scalable deployment across diverse patient groups. Investigating effective transfer learning protocols thus represents a critical avenue for advancing AI-driven rehabilitation technologies.

(5) Investigating RL approaches: the review shows that few studies have applied RL in rehabilitation settings, and those that do often lack comprehensive validation [55, 58, 59, 66]. This limited adoption is likely due to several key challenges, including safety concerns when deploying RL algorithms in clinical environments, the absence of reliable and realistic simulation platforms to adequately train and test RL agents before involving human subjects, and issues related to sample efficiency, which hinder learning from limited patient data. Additionally, the limited adoption of RL in rehabilitation settings is also influenced by the inherent challenges related to simulating physiological signals and patient responses. Unlike many other application domains, rehabilitation involves complex, highly individualized physiological processes that are difficult to model accurately. Each patient's biological and neurological responses to interventions vary significantly, making it nearly impossible to create reliable simulation environments that can predict how a subject's physiological state will change in response to specific actions taken by the RL agent. This lack of realistic and patient-specific simulators complicates the training and validation of RL algorithms before deployment in clinical settings, as the system cannot fully anticipate the consequences of its decisions on a real patient's health. As a result, the physiological side of the patient is essentially unmodelable in a comprehensive way, posing a critical barrier to safe and effective RL application in rehabilitation. Addressing this challenge requires innovative approaches that either improve simulation fidelity or develop safe on-line learning frameworks capable of adapting in real time while minimizing risk. Future research should therefore focus on a deeper exploration and transparent reporting of RL methodologies with particular attention to safety, clinical relevance, and translational potential. Important issues to address include:
   - the safe integration of RL into rehabilitation systems with guarantees for patient safety;
   - the development of simulation environments necessary to thoroughly test RL algorithms before clinical trials, particularly addressing the challenge of realistically modeling individualized physiological responses;
   - strategies to improve simulation fidelity to better capture patient-specific physiological dynamics or, alternatively, the creation of safe online learning frameworks that allow RL agents to adapt in real time with minimal risk;
   - approaches to enhance sample efficiency in order to enable effective RL training despite the limited availability of clinical data;
   - the establishment of standardized protocols for evaluating and reporting the safety and efficacy of RL applications in clinical rehabilitation settings.

By addressing these questions, the scientific community can advance the field of AI-driven upper limb robot-aided rehabilitation, ensuring that these technologies are both effective and safe for clinical use.

5 Conclusions

This systematic review has been conducted to provide an overview of the application of data-driven AI approaches in robot-aided upper limb rehabilitation. Specifically, it examines how different learning paradigms, task types, and model types, ranging from ML to DL, have been adopted in the literature. The goal is to outline the current state of research and to support the integration of intelligent, adaptive AI modules into robotic rehabilitation systems.

Considering the PRISMA method and the inclusion criteria, 35 works have been included, dividing their discussion according to the specific AI-driven functional block: UIR, RMP, RIC, and SA. Four tables are presented to detail the research studies and the AI approaches implemented in the literature. A bar chart has been generated to have a better idea about the algorithms used. It emerged that the classification problems have a higher occurrence, and they are faced with implementing ML methods. On the other hand, DL is mostly implemented to face regression and reinforcement tasks. Additionally, a parallel categories plot has been added to provide a multi-dimensional view of the studies, highlighting variability in functional modules, algorithms, and performance metrics, and revealing the challenges in comparing methodologies due to a lack of standardization.

The systematic review findings emphasize the profound influence of AI on reshaping upper limb robot-aided rehabilitation, tailoring AI methodologies to diverse fields. The extensive AI applications in UIR, RMP, RIC, and SA offer substantial potential for enhancing rehabilitation outcomes of upper limb impairment. Yet, limited validation exists for subjects with neuromuscular or musculoskeletal conditions. Nonetheless, sustained research and development are imperative to fully harness the potential of AI within this pivotal healthcare domain.

Acknowledgment

Rita Molle is a PhD student enrolled in the National PhD in Artificial Intelligence, XXXVIII cycle, course on Health and Life Sciences, organized by Università Campus Bio-Medico di Roma.

References

[1] Ziyi Yang, Shuxiang Guo, Yi Liu, Hideyuki Hirata, and Takashi Tamiya. 2021. An intention-based online bilateral training system for upper limb motor rehabilitation. *Microsystem Technologies* 27 (2021), 211–222.

[2] Lincong Luo, Liang Peng, Chen Wang, and Zeng-Guang Hou. 2019. A greedy assist-as-needed controller for upper limb rehabilitation. *IEEE Transactions on Neural Networks and Learning Systems* 30, 11 (2019), 3433–3443.

[3] Roberto Colombo, Fabrizio Pisano, Silvestro Micera, Alessandra Mazzone, Carmen Delconte, M. Chiara Carrozza, Paolo Dario, and Giuseppe Minuco. 2005. Robotic techniques for upper limb evaluation and rehabilitation of stroke patients. *IEEE Transactions on Neural Systems and Rehabilitation Engineering* 13, 3 (2005), 311–324.

[4] Helen Rodgers, Helen Bosomworth, Hermano I. Krebs, Frederike van Wijck, Denise Howel, Nina Wilson, Lydia Aird, Natasha Alvarado, Sreeman Andole, David L. Cohen, et al. 2019. Robot assisted training for the upper limb after stroke (RATULS): A multicentre randomised controlled trial. *Lancet* 394, 10192 (2019), 51–62.

[5] Christian Tamantini, Francesca Cordella, Clemente Lauretti, Francesco Scotto Di Luzio, Benedetta Campagnola, Laura Cricenti, Marco Bravi, Federica Bressi, Francesco Draicchio, Silvia Sterzi, et al. 2023. Tailoring upper-limb robot-aided orthopedic rehabilitation on patients' psychophysiological state. *IEEE Transactions on Neural Systems and Rehabilitation Engineering* 31 (2023), 3297–3306.

[6] Ritwika Choudhuri, John Solomon, Aravind Nehrujee, S. Sujatha, and Sivakumar Balasubramanian. 2025. *Effect of Role of Robotic Assistance on Upper-Limb Sensorimotor Recovery: A Systematic Review and Meta-Analysis*. medRxiv, 2025-04. Retrieved from https://www.medrxiv.org/content/10.1101/2025.04.24.25326375v1

[7] Vincenzo Di Lazzaro, Fioravante Capone, Giovanni Di Pino, Giovanni Pellegrino, Lucia Florio, Loredana Zollo, Davide Simonetti, Federico Ranieri, Nicoletta Brunelli, Marzia Corbetto, et al. 2016. Combining robotic training and non-invasive brain stimulation in severe upper limb-impaired chronic stroke patients. *Frontiers in Neuroscience* 10 (2016), 88.

[8] Rita Molle, Christian Tamantini, Clemente Lauretti, Emilio Maria Romano, and Loredana Zollo. 2025. An online reinforcement learning method to improve control adaptability in robot-aided rehabilitation. *Engineering Applications of Artificial Intelligence* 161 (2025), 112248.

[9] Bu Hyun Yoon, Chanhee Park, and Joshua (Sung) Hyun You. 2022. Minimal contact robotic stroke rehabilitation on risk of Covid-19. *Work Efficiency and Sensorimotor Function* 10, 4 (2022), 691.

[10] Nicholas Flynn, Elspeth Froude, Deirdre Cooke, and Suzanne Kuys. 2022. Repetitions, duration and intensity of upper limb practice following the implementation of robot assisted therapy with sub-acute stroke survivors: An observational study. *Disability and Rehabilitation. Assistive Technology* 17, 6 (2022), 675–680.

[11] Christian Tamantini, Kevin Patrice Langlois, Joris de Winter, Parham Haji Ali Mohamadi, David Beckwée, Eva Swinnen, Tom Verstraten, Bram Vanderborght, and Loredana Zollo. 2025. Promoting active participation in robot-aided rehabilitation via machine learning and impedance control. *Frontiers in Digital Health* 7 (2025), 1559796.
[12] Luke Hampshire, Abbas Dehghani-Sanij, and Rory James O'Connor. 2022. Restorative rehabilitation robotics to promote function, independence and dignity: Users' perspectives on clinical applications. *Journal of Medical Engineering & Technology* 46, 6 (2022), 527–535.
[13] Jiaze He and Ting Yang. 2022. In the era of long covid, can we seek new techniques for better rehabilitation? *Chronic Diseases and Translational Medicine* 8, 3 (2022), 149–153.
[14] Francesco Lanotte, Megan K. O'Brien, and Arun Jayaraman. 2023. AI in rehabilitation medicine: Opportunities and challenges. *Annals of Rehabilitation Medicine* 47, 6 (2023), 444.
[15] Christian Tamantini, Francesco Scotto di Luzio, Claudiu Daniel Hromei, Lorenzo Cristofori, Danilo Croce, Marco Cammisa, Arcangela Cristofaro, Maria Vittoria Marabello, Roberto Basili, and Loredana Zollo. 2023. Integrating physical and cognitive interaction capabilities in a robot-aided rehabilitation platform. *IEEE Systems Journal* 17 (2023), 6516–6527.
[16] Mayank Kumar Danishta and Anchit Gugnani. 2025 Advancements in physiotherapy: A systematic review of AI, robotics and wearable sensor technologies. *International Journal for Multidisciplinary Research* 7 (2025), 1–9.
[17] Clautilde Nguiadem, Maxime Raison, and Sofiane Achiche. 2020. Motion planning of upper-limb exoskeleton robots: A review. *Applied Sciences* 10, 21 (2020), 7626.
[18] Abolfazl Mohebbi. 2020. Human-robot interaction in rehabilitation and assistance: A review. *Current Robotics Reports* 1 (2020), 131–144.
[19] Jyotindra Narayan, Bhaben Kalita, and Santosha Kumar Dwivedy. 2021. Development of robot-based upper limb devices for rehabilitation purposes: A systematic review. *Augmented Human Research* 6 (2021), 1–33.
[20] Manuel Andrés Vélez-Guerrero, Mauro Callejas-Cuervo, and Stefano Mazzoleni. 2021. Artificial intelligence-based wearable robotic exoskeletons for upper limb rehabilitation: A review. *Sensors* 21, 6 (2021), 2146.
[21] Luzheng Bi and Cuntai Guan. 2019. A review on EMG-based motor intention prediction of continuous human upper limb motion for human-robot collaboration. *Biomedical Signal Processing and Control* 51 (2019), 113–127.
[22] Omar Coser, Christian Tamantini, Paolo Soda, and Loredana Zollo. 2024. AI-based methodologies for exoskeleton-assisted rehabilitation of the lower limb: A review. *Frontiers in Robotics and AI* 11 (2024), 1341580.
[23] Dezhen Xiong, Daohui Zhang, Xingang Zhao, and Yiwen Zhao. 2021. Deep learning for EMG-based human-machine interaction: A review. *IEEE/CAA Journal of Automatica Sinica* 8, 3 (2021), 512–533.
[24] Pankaj Dhatrak, Jeet Durge, Rahul Kumar Dwivedi, Haresh Kumar Pradhan, and Sona Kolke. 2024. Interactive design and challenges on exoskeleton performance for upper-limb rehabilitation: A comprehensive review. *International Journal on Interactive Design and Manufacturing* 19 (2024), 1–23.
[25] Qingsong Ai, Zemin Liu, Wei Meng, Quan Liu, and Sheng Q. Xie. 2021. Machine learning in robot-assisted upper limb rehabilitation: A focused review. *IEEE Transactions on Cognitive and Developmental Systems* 15, 4 (2021), 2053–2063.
[26] Christian Tamantini, Alessandro Umbrico, and Andrea Orlandini. 2025. Automated planning and scheduling in robot-aided rehabilitation: A review. *Journal of NeuroEngineering and Rehabilitation* 22, 1 (2025), 180.
[27] Yuexing Gu, Yuanjing Xu, Yuling Shen, Hanyu Huang, Tongyou Liu, Lei Jin, Hang Ren, and Jinwu Wang. 2022. A review of hand function rehabilitation systems based on hand motion recognition devices and artificial intelligence. *Brain Sciences* 12, 8 (2022), 1079.
[28] Zulikha Ayomikun Adeola-Bello and Norsinnira Zainul Azlan. 2022. Power assist rehabilitation robot and motion intention estimation. *International Journal of Robotics and Control Systems* 2, 2 (2022), 297–316.
[29] Wei Xiao, Kai Chen, Jiaming Fan, Yifan Hou, Weifei Kong, and Guo Dan. 2023. AI-driven rehabilitation and assistive robotic system with intelligent PID controller based on RBF neural networks. *Neural Computing and Applications* 35, 22 (2023), 16021–16035.
[30] Francisco J. Badesa, Ricardo Morales, Nicolas Garcia-Aracil, José María Sabater, Alicia Casals, and Loredana Zollo. 2014. Auto-adaptive robot-aided therapy using machine learning techniques. *Computer Methods and Programs in Biomedicine* 116, 2 (2014), 123–130.
[31] David Moher, Alessandro Liberati, Jennifer Tetzlaff, and Douglas G. Altman, and PRISMA Group. 2009. Preferred reporting items for systematic reviews and meta-analyses: The Prisma statement. *Annals of Internal Medicine* 151, 4 (2009), 264–269.
[32] Mindy F. Levin and Marika Demers. 2021. Motor learning in neurological rehabilitation. *Disability and Rehabilitation* 43, 24 (2021), 3445–3453.
[33] Xiangyun Li, Qi Lu, Peng Chen, Shan Gong, Xi Yu, Hongchen He, and Kang Li. 2023. Assistance level quantification-based human-robot interaction space reshaping for rehabilitation training. *Frontiers in Neurorobotics* 17 (2023), 1161007.
[34] Qingling Li and Yu Song. 2012. SEMG control of an upper limb rehabilitation robot based on boosting of neural networks. In *2012 IEEE International Conference on Mechatronics and Automation*. IEEE, 428–433.

[35] Kai Gui, Honghai Liu, and Dingguo Zhang. 2019. A practical and adaptive method to achieve EMG-based torque estimation for a robotic exoskeleton. *IEEE/ASME Transactions on Mechatronics* 24, 2 (2019), 483–494.

[36] Hao Liu, Jun Tao, Pan Lyu, and Fang Tian. 2020. Human-robot cooperative control based on sEMG for the upper limb exoskeleton robot. *Robotics and Autonomous Systems* 125 (2020), 103350.

[37] Biao Chen, Yang Zhou, Chaoyang Chen, Zain Sayeed, Jie Hu, Jin Qi, Todd Frush, Henry Goitz, John Hovorka, Mark Cheng, et al. 2023. Volitional control of upper-limb exoskeleton empowered by EMG sensors and machine learning computing. *Array* 17 (2023), 100277.

[38] Siqi Cai, Yan Chen, Shuangyuan Huang, Yan Wu, Haiqing Zheng, Xin Li, and Longhan Xie. 2019. SVM-based classification of sEMG signals for upper-limb self-rehabilitation training. *Frontiers in Neurorobotics* 13 (2019), 31.

[39] Triwiyanto Triwiyanto, Wahyu Caesarendra, Vugar Abdullayev, Abdussalam Ali Ahmed, and Herianto Herianto. 2023. Single lead EMG signal to control an upper limb exoskeleton using embedded machine learning on raspberry Pi. *Journal of Robotics and Control* 4, 1 (2023), 35–45.

[40] Ismail Mohd Khairuddin, Shahrul Naim Sidek, Anwar P. P. Abdul Majeed, Mohd Azraai Mohd Razman, Asmarani Ahmad Puzi, and Hazlina Md Yusof. 2021. The classification of movement intention through machine learning models: The identification of significant time-domain EMG features. *PeerJ Computer Science* 7 (2021), e379.

[41] Bridget Schabron, Jaydip Desai, and Yimesker Yihun. 2021. Wheelchair-mounted upper limb robotic exoskeleton with adaptive controller for activities of daily living. *Sensors* 21, 17 (2021), 5738.

[42] Benzhen Guo, Yanli Ma, Jingjing Yang, Zhihui Wang, and Xiao Zhang. 2020. Lw-CNN-based myoelectric signal recognition and real-time control of robotic arm for upper-limb rehabilitation. *Computational Intelligence and Neuroscience* 2020 (2020), 8846021.

[43] Craig G. McDonald, Jennifer L. Sullivan, Troy A. Dennis, and Marcia K. O'Malley. 2020. A myoelectric control interface for upper-limb robotic rehabilitation following spinal cord injury. *IEEE Transactions on Neural Systems and Rehabilitation Engineering* 28, 4 (2020), 978–987.

[44] Luis G. Hernández and Javier M. Antelis. 2019. Self-paced movement intention recognition from EEG signals during upper limb robot-assisted rehabilitation. In *2019 9th International IEEE/EMBS Conference on Neural Engineering (NER)*. IEEE, 69–72.

[45] Ji-Hoon Jeong, Kyung-Hwan Shim, Dong-Joo Kim, and Seong-Whan Lee. 2020. Brain-controlled robotic arm system based on multi-directional CNN-BiLSTM network using EEG signals. *IEEE Transactions on Neural Systems and Rehabilitation Engineering* 28, 5 (2020), 1226–1238.

[46] Hui Tian. 2024. Human-robot interaction in motor imagery: A system based on the STFCN for unilateral upper limb rehabilitation assistance. *Journal of Neuroscience Methods* 411 (2024), 110240.

[47] Yonghao Song, Siqi Cai, Lie Yang, Guofeng Li, Weifeng Wu, and Longhan Xie. 2020. A practical EEG-based human-machine interface to online control an upper-limb assist robot. *Frontiers in Neurorobotics* 14 (2020), 32.

[48] Antonio Frisoli, Claudio Loconsole, Daniele Leonardis, Filippo Banno, Michele Barsotti, Carmelo Chisari, and Massimo Bergamasco. 2012. A new gaze-BCI-driven control of an upper limb exoskeleton for rehabilitation in real-world tasks. *IEEE Transactions on Systems, Man, and Cybernetics, Part C (Applications and Reviews)* 42, 6 (2012), 1169–1179.

[49] Peter Martin and M. Reza Emami. 2014. A neuro-fuzzy approach to real-time trajectory generation for robotic rehabilitation. *Robotics and Autonomous Systems* 62, 4 (2014), 568–578.

[50] Jia-Liang Ren, Ya-Hui Chien, En-Yu Chia, Li-Chen Fu, and Jin-Shin Lai. 2019. Deep learning based motion prediction for exoskeleton robot control in upper limb rehabilitation. In *2019 International Conference on Robotics and Automation (ICRA)*. IEEE, 5076–5082.

[51] Quan Liu, Yang Liu, Yi Li, Chang Zhu, Wei Meng, Qingsong Ai, and Sheng Q. Xie. 2021. Path planning and impedance control of a soft modular exoskeleton for coordinated upper limb rehabilitation. *Frontiers in Neurorobotics* 15 (2021), 745531.

[52] He Li, Shuxiang Guo, Dongdong Bu, Hanze Wang, and Masahiko Kawanishi. 2023. Subject-independent estimation of continuous movements using CNN-LSTM for a home-based upper limb rehabilitation system. *IEEE Robotics and Automation Letters* 8 (2023), 6403–6410.

[53] Beatrice Luciani, Loris Roveda, Francesco Braghin, Alessandra Pedrocchi, and Marta Gandolla. 2023. Trajectory learning by therapists' demonstrations for an upper limb rehabilitation exoskeleton. *IEEE Robotics and Automation Letters* 8, 8 (2023), 4561–4568.

[54] Peimin Xie, Shuangyuan Huang, Chen Lv, and Longhan Xie. 2024. Imitation learning control strategy based on probabilistic motor primitive for upper limb rehabilitation training. In *2024 IEEE International Conference on Cybernetics and Intelligent Systems (CIS) and IEEE International Conference on Robotics, Automation and Mechatronics (RAM)*. IEEE, 1–6.

[55] Xusheng Wang, Jiexin Xie, Shijie Guo, Yue Li, Pengfei Sun, and Zhongxue Gan. 2021. Deep reinforcement learning-based rehabilitation robot trajectory planning with optimized reward functions. *Advances in Mechanical Engineering* 13, 12 (2021), 16878140211067011.

[56] Jiang Hua, Liangcai Zeng, Gongfa Li, and Zhaojie Ju. 2021. Learning for a robot: Deep reinforcement learning, imitation learning, transfer learning. *Sensors* 21, 4 (2021), 1278.

[57] Guozheng Xu, Aiguo Song, and Huijun Li. 2011. Adaptive impedance control for upper-limb rehabilitation robot using evolutionary dynamic recurrent fuzzy neural network. *Journal of Intelligent & Robotic Systems* 62 (2011), 501–525.

[58] Zaid Al-Jumaili, Tanjulee Siddique, Raouf Fareh, Mahmoud A. Y. Abdallah, Mahafuzur Rahaman Khan, Mohammad Habibur Rahman, and Maamar Bettayeb. 2023. Reinforcement learning-based control for an upper limb rehabilitation robot. In *2023 Advances in Science and Engineering Technology International Conferences (ASET)*. IEEE, 1–6.

[59] Fancheng Meng and Yaping Dai. 2014. Adaptive inverse optimal control for rehabilitation robot systems using actor-critic algorithm. *Mathematical Problems in Engineering* 2014 (2014), 1–15.

[60] Qingcong Wu, Xingsong Wang, Bai Chen, and Hongtao Wu. 2018. Development of an RBFN-based neural-fuzzy adaptive control strategy for an upper limb rehabilitation exoskeleton. *Mechatronics* 53 (2018), 85–94.

[61] Rhythm Arora, Matteo Lavit Nicora, Pooja Prajod, Daniele Panzeri, Elisabeth André, Patrick Gebhard, and Matteo Malosio. 2022. Employing socially interactive agents for robotic neurorehabilitation training. arXiv:2206.01587. Retrieved from https://arxiv.org/abs/2206.01587

[62] Domen Novak, Matjaž Mihelj, Jaka Ziherl, Andrej Olensek, and Marko Munih. 2011. Psychophysiological measurements in a biocooperative feedback loop for upper extremity rehabilitation. *IEEE Transactions on Neural Systems and Rehabilitation Engineering* 19, 4 (2011), 400–410.

[63] WenDong Wang, JunBo Zhang, Xin Wang, XiaoQing Yuan, and Peng Zhang. 2022. Motion intensity modeling and trajectory control of upper limb rehabilitation exoskeleton robot based on multi-modal information. *Complex & Intelligent Systems* 8, 3 (2022), 2091–2103.

[64] Siqi Cai, Xuyang Wei, Enze Su, Weifeng Wu, Haiqing Zheng, and Longhan Xie. 2020. Online compensation detecting for real-time reduction of compensatory motions during reaching: A pilot study with stroke survivors. *Journal of Neuroengineering and Rehabilitation* 17 (2020), 1–11.

[65] Siqi Cai, Guofeng Li, Enze Su, Xuyang Wei, Shuangyuan Huang, Ke Ma, Haiqing Zheng, and Longhan Xie. 2020. Real-time detection of compensatory patterns in patients with stroke to reduce compensation during robotic rehabilitation therapy. *IEEE Journal of Biomedical and Health Informatics* 24, 9 (2020), 2630–2638.

[66] Patricia Kan, Rajibul Huq, Jesse Hoey, Robby Goetschalckx, and Alex Mihailidis. 2011. The development of an adaptive upper-limb stroke rehabilitation robotic system. *Journal of Neuroengineering and Rehabilitation* 8, 1 (2011), 1–18.

[67] Luis Bote Curiel, Sergio Munoz-Romero, Alicia Gerrero-Curieses, and José Luis Rojo-Álvarez. 2019. Deep learning and big data in healthcare: A double review for critical beginners. *Applied Sciences* 9, 11 (2019), 2331.

[68] Iqbal H. Sarker. 2021. Deep learning: A comprehensive overview on techniques, taxonomy, applications and research directions. *SN Computer Science* 2, 6 (2021), 420.

[69] Pham Van Cuong and Wang Yao Nan. 2016. Adaptive trajectory tracking neural network control with robust compensator for robot manipulators. *Neural Computing and Applications* 27 (2016), 525–536.

[70] Vesna D. Novak, Alexander C. Koenig, and Robert Riener. 2022. Psychophysiological integration of humans and machines for rehabilitation. In *Neurorehabilitation Technology*. D. J. Reinkensmeyer, L. Marchal-Crespo, and V. Dietz (Eds.), Springer, 207–221.

[71] Rita Molle, Christian Tamantini, Clemente Lauretti, Francesca Cordella, Francesco Scotto di Luzio, Davide Sebastiani, Fabio Santacaterina, Marco Bravi, Federica Bressi, Sandra Miccinilli, et al. 2025. Exploring priority parameters in physiotherapist decision models for tailoring robot-aided rehabilitation. *International Journal of Social Robotics* (2025), 1–16. DOI: https://doi.org/10.1007/s12369-025-01309-3

Received 24 February 2025; revised 27 October 2025; accepted 2 December 2025